

Final Report

Permanent-Change Thermal Paints for Hypersonic Flight-Test

AFOSR/AOARD Reference Number: AOARD-09-4025

AFOSR/AOARD Program Manager: Pon R. Ponnappan

Period of Performance: 2009/04/23 – 2010/09/13

Submission Date: 13 September 2010

Principal Investigators:

Andrew J. Neely, Hans Riesen, University of New South Wales

This report includes contributions from Katie Kruger, Rishabh Choudhury, Jack Appleton, Phil Tracy, Wei Tjong, Ayhan Yesil, Daniel Paukner, Robert Clark and Harriet Cameron.



UNSW@ADFA
CANBERRA • AUSTRALIA

Report Documentation Page		Form Approved OMB No. 0704-0188
Public reporting burden for the collection of information is estimated to average 1 hour per response, including the time for reviewing instructions, searching existing data sources, gathering and maintaining the data needed, and completing and reviewing the collection of information. Send comments regarding this burden estimate or any other aspect of this collection of information, including suggestions for reducing this burden, to Washington Headquarters Services, Directorate for Information Operations and Reports, 1215 Jefferson Davis Highway, Suite 1204, Arlington VA 22202-4302. Respondents should be aware that notwithstanding any other provision of law, no person shall be subject to a penalty for failing to comply with a collection of information if it does not display a currently valid OMB control number.		
1. REPORT DATE 24 SEP 2010	2. REPORT TYPE Final	3. DATES COVERED 23-04-2009 to 16-09-2010
4. TITLE AND SUBTITLE Thermal Paints for Hypersonic Flight-Test		5a. CONTRACT NUMBER FA23860914025
		5b. GRANT NUMBER
		5c. PROGRAM ELEMENT NUMBER
6. AUTHOR(S) Andrew Neely		5d. PROJECT NUMBER
		5e. TASK NUMBER
		5f. WORK UNIT NUMBER
7. PERFORMING ORGANIZATION NAME(S) AND ADDRESS(ES) University of New South Wales,Northcott Drive,Canberra ACT 2600,Australia,NA,NA		8. PERFORMING ORGANIZATION REPORT NUMBER N/A
9. SPONSORING/MONITORING AGENCY NAME(S) AND ADDRESS(ES) AOARD, UNIT 45002, APO, AP, 96337-5002		10. SPONSOR/MONITOR'S ACRONYM(S) AOARD-094025
		11. SPONSOR/MONITOR'S REPORT NUMBER(S)
12. DISTRIBUTION/AVAILABILITY STATEMENT Approved for public release; distribution unlimited		
13. SUPPLEMENTARY NOTES		
14. ABSTRACT This report describes the ongoing work performed over the last 18 months on the investigation of the use of permanent-change thermal paints for mapping structural heating during hypersonic flight tests. This technique has a number of practical advantages of other established thermal mapping methods including the low cost and overhead associated with the application of these coatings to a flight vehicle and the ease of good spatial coverage. Techniques to identify the components and analyze the chemical behavior of these paints analyze and have been established and demonstrated and these are reported in detail. An investigation of the pressure dependence of the paint response is described but has to date been inconclusive and is ongoing. Numerically based techniques have been established and demonstrated to model the full transient heating of the vehicle across its trajectory. These methods can account for the fluid-thermal-structural interactions associated with the aerothermodynamics heating of the vehicle and its structural response. These simulations have successfully been applied to the critical portion of the atmospheric descent of the HIFiRE-0 payload. The numerical techniques and initial simulations are described. A practical laboratory-based method of reproducing the transient heating histories representative of flight has been developed and demonstrated. This incorporates a computer-controlled high-power TIG welder to heat the sample via an electric arc. This heating method can be applied to non-metallic samples via the use of a target heat sink placed in thermal contact with sample and this has been successfully demonstrated. Thermal paint coatings have been successfully applied to HIFiRE-0 vehicle and flown. Clear color change was evident in regions of high heating and this conforms well to initial estimates. This initial analysis of color change on the recently recovered HIFiRE-0 payload is described although this work is still at an early stage.		

15. SUBJECT TERMS					
16. SECURITY CLASSIFICATION OF:			17. LIMITATION OF ABSTRACT Same as Report (SAR)	18. NUMBER OF PAGES 48	19a. NAME OF RESPONSIBLE PERSON
a. REPORT unclassified	b. ABSTRACT unclassified	c. THIS PAGE unclassified			

DISCLAIMER

Any opinions expressed in this report are those of the authors and are not necessarily the views of the University of New South Wales or any other external organisation.

Abstract

This report describes the ongoing work performed over the last 18 months on the investigation of the use of permanent-change thermal paints for mapping structural heating during hypersonic flight tests. This technique has a number of practical advantages of other established thermal mapping methods including the low cost and overhead associated with the application of these coatings to a flight vehicle and the ease of good spatial coverage. Techniques to identify the components and analyse the chemical behaviour of these paints have been established and demonstrated and these are reported in detail. An investigation of the pressure dependence of the paint response is described but has to date been inconclusive and is ongoing. Numerically based techniques have been established and demonstrated to model the full transient heating of the vehicle across its trajectory. These methods can account for the fluid-thermal-structural interactions associated with the aerothermodynamic heating of the vehicle and its structural response. These simulations have successfully been applied to the critical portion of the atmospheric descent of the HIFiRE-0 payload. The numerical techniques and initial simulations are described. A practical laboratory-based method of reproducing the transient heating histories representative of flight has been developed and demonstrated. This incorporates a computer-controlled high-power TIG welder to heat the sample via an electric arc. This heating method can be applied to non-metallic samples via the use of a target heat sink placed in thermal contact with sample and this has been successfully demonstrated. Thermal paint coatings have been successfully applied to HIFiRE-0 vehicle and flown. Clear colour change was evident in regions of high heating and this conforms well to initial estimates. This initial analysis of colour change on the recently recovered HIFiRE-0 payload is described although this work is still at an early stage.

Objectives

The overall objective of this research project was to develop and demonstrate a methodology for performing quantitative global temperature measurements on vehicle structures that have undergone hypersonic flight test.

The specific objectives were to:

- Investigate the paint chemistry and use spectroscopic measurements to determine the rate constants and activation energies of the colour-change reactions for the different paint mixtures. This had not previously been attempted for this class of paints as it has for TSPs.
- Investigate and develop an analytical model to predict an end paint colour from a predicted surface temperature history based on the Arrhenius constants.
- Establishment of candidate heating histories representative of those experienced by the vehicle structure during hypersonic flight.
- Develop a controllable method of accurately reproducing predicted surface temperature histories on painted samples in the lab using CW laser heating.
- Determine the overall levels of uncertainty of these measurements by directly comparing temperature history predictions based on final paint colour with the measured temperature histories used to induce the colour change.

Additionally it was intended to pursue the following two objectives, which while sitting outside the basic science of the proposal will begin to address some of the engineering aspects of the technique:

- Test fly patches of paint under hypersonic test conditions (possibly on HIFiRE-0) to investigate the application methods, site selections and paint survivability in-flight and on impact. This will also provide an initial test case for post recovery handling and analysis of the painted surfaces.
- Investigate the bonding of the paints to a range of materials and surface finishes under erosive high heat-flux conditions produced by the oxy-torch and strategies for the illumination and filming of internal painted surfaces for inclusion during flight tests.

Table of Contents

ABSTRACT	I
OBJECTIVES	II
TABLE OF CONTENTS	III
TABLE OF FIGURES	V
BACKGROUND	1
GLOBAL THERMAL MEASUREMENT TECHNIQUES	2
Discrete sensor arrays	2
Thermochromic liquid crystals	2
Infrared thermography	2
TSPs and thermal phosphors	3
Permanent-change thermal paints	3
Summary	3
CALIBRATION STRATEGIES	4
TRANSIENT HEATING CALIBRATION RIG	5
Oxy-acetylene torch heating	5
Electrical resistance heating	7
Laser-based radiative heating	8
Electric-arc based heating	9
Data capture during transient heating experiments	12
CHEMISTRY OF THE PERMANENT-CHANGE THERMAL PAINTS	14
Elemental analysis of paints using X-ray fluorescence	15

Monitoring chemical changes via IR transmission spectroscopy	16
Spectrophotometer measurements	17
Limitations of spectral analysis	19
Pressure dependence of paint response	19
THERMAL MODELLING OF TRAJECTORY HEATING	21
Fluid-structure interaction approach	22
CFD and FEM solution domains	22
Transient FSI Solutions	24
FLIGHT TESTING OF THE PERMANENT-CHANGE THERMAL PAINTS	27
HIFiRE-0 Flight Test Vehicle	27
Application of thermal paints to HIFiRE-0 vehicle	27
Post-flight analysis of paint response on HIFiRE-0	29
SUMMARY	32
FUTURE WORK	33
APPENDICES	34
Personnel Supported	34
Acknowledgements	34
Publications Resulting from this Project	35
Interactions	36
Allocation of the Budget	37
References	38

Table of Figures

Figure 1. (a) Schematic and (b) photograph of oxy-acetylene torch transient calibration setup showing the painted test plate, insulating brick, IR and CCD cameras and LED lights.	5
Figure 2. (a) Still image from IR camera history of transient calibration test showing regions of interest (ROIs) with (b) matching surface temperature histories at various radial locations outwards from the centre of heating.	6
Figure 3. (a) Colour change for SC275 thermal paint during transient heating with oxy-acetylene torch. (b) Data collection regions. (c) Histories of HSV and temperature data for region 1.	6
Figure 4. (a) Thermal image of the thin bow tie and power supply cables. The painted coupon reached a maximum of 505°C, (b) post-heating distribution of paint colour (MC165-2) on the coupon after the calibration.	7
Figure 5. Temperature history for resistive heating of painted KANTHAL-AF bow-tie samples of different thicknesses.	8
Figure 6. Radiative heating using a CO ₂ laser illuminating either the front or rear surface of the painted sample.	9
Figure 7. Schematic of electric-arc based calibration rig	10
Figure 8. Detail of sample mounting with the addition of a target heat sink	10
Figure 9. Testing of the target heat sinks (a) experimental lay out, close up of the (b) 2mm thick and (c) 10 mm thick copper target heat sinks centrally located on the mild steel sample plates.	11
Figure 10. Comparison of (a) FEM predictions of radial temperature distribution across the backside of the sample plate in perfect thermal contact with a range of cylindrical copper target heat sinks with (b) experimental measurement of the temperature distributions for a higher power setting.	11
Figure 11. Infrared thermograms and temperature distributions across the 150x150x1.6 mm mild steel plate (a) with no target heat sink and (b) with a 25 mm diameter x 2.5 mm deep copper target heat sink. The red region-of-interest line	12
Figure 12. Fibre-optic visible spectrometer measurements of colour transition during transient heating of painted sample.	13
Figure 13. Calibration colour maps for the single-change paints: SC155, SC240, SC275, SC367, SC400, SC458, SC550, SC630. (Neely & Tracy 2006) Note that this digital images have not been colour corrected.	14
Figure 14. Calibration colour maps for the multi-change paints: MC135-2, MC165-2, MC395-3, MC490-10, MC520-7. (Neely & Tracy 2006) Note that this digital images have not been colour corrected.	15
Figure 15. Example x-ray fluorescence spectra for (a) SC275 and (b) MC490-10	16
Figure 16. IR transmission spectra measured for SC155 after heating at 155 °C for a range of times.	17
Figure 17. Measurements of colour response of SC155 samples exposed to oven heating from 20°C to 200°C using spectrophotometer. (a) Reflectance spectra and (b) absorbance spectra.	18
Figure 18. Absorbance vs. temperature of SC155 for various wavelengths from 400nm to 700nm.	18
Figure 19. Pressure testing of thermal paint response.	20
Figure 20. Before and after colour comparison of the pressure test samples: (a) spectra of samples (b) samples.	20
Figure 21. Variation of (a) freestream density, (b) freestream velocity, (c) ratio of wall to total enthalpy and (d) stagnation heat flux for a 10-second descent from 50 km at Mach 7.	22

Figure 22. Solid model of the vehicle showing detail of the nose cone tip for the 3522 element FEM mesh.	23
Figure 23. CFD domain used to model the flow field over the HIFiRE-0 vehicle. Inserts show detail of the mesh in the vicinity of the nose cone tip.	24
Figure 24. CFD flow field solution showing detail of Mach number distribution near the tip of the nose cone at 50 km altitude and a flight speed of 2321 m/s.	24
Figure 25. (a) Temperature distribution, °C and (b) stress distribution, Pa in the nose cone tip after a 10-second descent from 50 km to 28 km.	25
Figure 26. Surface temperature histories at three locations along the vehicle during the 10-second descent from 50 km to 28 km.	25
Figure 27. Mach number distribution in the external flow and temperature distribution in the HIFiRE-0 vehicle structure calculated from transient FSI simulations.	26
Figure 28. Temperature distribution along the surface of the HIFiRE-0 vehicle structure after descent through the atmosphere.	26
Figure 29. Layout of the modelled front section of the HIFiRE-0 vehicle.	27
Figure 30. Paint scheme on the HIFiRE-0 vehicle showing patches of single-change and multi-change thermal paint on external and internal surfaces of the stainless steel nose cone and around the external camera mount on the instrument can (photos courtesy of DSTO).	28
Figure 31. HIFiRE-0 on the launch rail at the Woomera test range showing detail of the thermal paint coatings (photos courtesy of DSTO).	29
Figure 32. Views of the MC165-2 and MC490-10 permanent-change thermal paints applied to the dummy camera mount and its immediate surroundings including the frame of the patch antenna. (a) pre-flight paint condition and (b) post-flight paint condition showing significant colour change on the MC165-2 paint and corrosion of the aluminium dummy camera mount. Paint change schemes are shown for reference (photos courtesy of DSTO).	30
Figure 33. Close up of the patch antenna mount on the recovered debris from the HIFiRE-0 vehicle showing the colour change on the MC490-10 paint on the stainless steel mounting frame. Note that the dummy camera mount is no longer attached in these images. (photos courtesy of DSTO).	30
Figure 34. (a) Measurement of paint thickness post flight on recovered components.	31
Figure 35. Transient simulation of the heating around the patch antenna mount on the aluminium instrumentation can. High levels of heating are visible along the overhanging edges of the stainless steel frame.	31

Background

We have been developing a methodology to quantify the transient response of permanent-change thermal paints for the mapping of structural temperatures on hypersonic flight-test vehicles. These thermal paints change colour as they undergo a chemical reaction as a function of temperature (Cowling *et al.* 1953). Unlike other coating-based methods for global temperature measurement such as thermochromic liquid crystals (Ireland *et al.* 1999, Ireland & Jones 2000), and temperature sensitive paints (Liu & Sullivan 2005), thermal paints are operable at the high structural temperatures (Lempereur *et al.* 2008) typical of a hypersonic vehicle and they undergo a permanent colour change that does not require in-situ illumination or imaging (Neely & Tjong 2008). These paints are an attractive, relatively low-cost and non-intrusive option to measure surface temperature distributions in regions of high thermal gradient such as occur for gap heating or due to corner flows around control surfaces and fin-fuselage junctions, shock boundary layer interactions, scramjet combustion chambers and around control thrusters. Thermal paints can also be applied to regions of the vehicle that cannot be easily instrumented by any other means. Data analysis requires either recovery of the vehicle or in-flight visualization of the painted surface. While these permanent-change thermal paints are available commercially for industrial use, particularly in the gas turbine industry where they have been largely developed (Bird *et al.* 1998, Lempereur *et al.* 2008) their transient response is not properly understood. In particular the final colour of the paint is a function of the temperature history and not just the maximum temperature of the surface to which they are applied (Kafka *et al.* 1965, Neely & Tracy 2006). We are working to establish the dependence of the chemical behaviour on the history of thermal input to the paint coating using controlled heating and spectroscopic measurements of the paint response for a series of commercially available single-change (SC) and multi-change (MC) paints. We are also developing calibration techniques that can induce a controlled surface temperature rise on painted samples in the short durations typical of HyShot-style ballistic flight tests.

Hypersonic research has been largely restricted to ground-based experiments due to the extreme cost of developing flight-test vehicles. The highly ambitious and successful Hyper-X program (McClinton 2006), enabled NASA to finally flight-test an operational airframe-integrated scramjet engine, but even with a deliberately small-scale vehicle the costs of the program were still immense. Other recent flight programs have aimed to perform short-duration experiments at atmospheric flight conditions but at minimal cost (Foelsche *et al.* 2005, Smart *et al.* 2006, Longo 2009).

While predictive methods are maturing and have been shown to provide good accuracy when compared to flight data (McClinton 2006, Leonard *et al.* 2005) there are still many uncertainties associated with the thermal modeling of the aero-structures of hypersonic vehicles. These largely relate to uncertainty in the fluid dynamics around the vehicle particularly in regions of shock impingement, gap heating and corner flows which in turn result in uncertainties in the heat transfer rates to be applied as boundary conditions in any thermal modelling (Edney 1956, Iliff & Shafer 1993, Leonard *et al.* 2005). It is thus crucial to comprehensively instrument flight vehicles to learn as much as possible about actual flight conditions so that predictive methods can be improved.

Flight weight restrictions often necessitate small structural margins, especially for non-reusable flight-test vehicles. The semi-monocoque design of most high-performance aerospace vehicles necessitates the use of the outer skin of the airframe as a main load-bearing structure. This outer skin is exposed to aerothermodynamic heating during flight and can quickly reach elevated temperature. All engineering materials degrade in mechanical performance at elevated temperature and this can be severe for the candidate materials and conditions for the airframes of hypersonic flight-test vehicles. To maintain structural mass limits it may even become necessary to operate the vehicle in a region of reduced strength or rigidity.

In the case of HyShot-style short-duration flights, extreme heating loads can result in highly transient structural temperatures. Here demands for usable payload fraction for the experiment and associated instrumentation can result in the aero-structure of the vehicle being driven toward probable thermally-induced mechanical failure by the end of the flight. Additionally, large temperature gradients in the airframe can induce significant stresses due to differential expansion, further compromising the design. This makes the ability to accurately predict heating rates and resultant airframe temperatures paramount.

Current HyShot trajectories use a ballistic lob to get the vehicle out of the atmosphere to reduce aerodynamic heating during acceleration to the test Mach number. These trajectories result in hypersonic atmospheric descents of the order of only 30 seconds duration (Smart *et al.* 2006) during which time the payload is subjected to aerodynamic heating. Heating can also pose a challenge on the ascent (Stewart *et al.* 2005). Whilst the payload is protected by a fairing or nose cone during the ascent, other parts of the airframe are still subjected to elevated temperatures which can compromise their structural integrity when also combined with extreme aerodynamic loads.

The FASST approach (Foelsche *et al.* 2005) takes a slightly different approach in that it launches the test vehicle along a suppressed ballistic trajectory that keeps the vehicle within the atmosphere during acceleration, resulting in slightly longer heat-soak durations of 30 seconds or more for the payload, which is initially protected by a shroud, and longer for the external airframe and aerodynamic surfaces. The Mach 10 HyCAUSE flight-test (Walker *et al.* 2005) used a higher ballistic trajectory to achieve a Mach 10 reentry and as a result reduce the atmospheric descent time to the order of just 10-15 seconds. It can be seen that any sensor system used to collect surface temperature data must be fast enough to respond during these short flight durations.

Global Thermal Measurement Techniques

Discrete sensor arrays

Structural temperatures and heating rates are usually obtained from a limited number of discrete sensors such as thermocouples or RTDs located at points of interest (Leonard *et al.* 2005). These sensors provide can provide accurate point temperature histories although they can be prone to signal interference such as RF. For high spatial resolution they must be employed in dense arrays but this is often restricted by mass and geometric considerations as well as available on-board data channels or telemetry bandwidth. The use of discrete wired sensors may also not practical on some locations on a hypersonic vehicle.

Thermochromic liquid crystals

Coatings of thermochromic liquid crystals (TLC) can provide a continuous and reversible history of temperature on a surface (Ireland & Jones 2000). These coatings selectively reflect white light due to the contraction and expansion of their helical chiral nematic (or cholesteric) molecular structure as a function of temperature. They are widely used in laboratory-based heat transfer experiments, particularly for gas turbine research, and in the medical and food industries. TLCs have been successfully used in low-speed flight tests to investigate transition on the exterior of a laminar flow nacelle (Bown *et al.* 1994) but they are not appropriate for hypersonic flight-test for two principle reasons: being reversible they require visualisation during the flight which is usually not practical, and they lack the robustness of thermal paints and are easily eroded, and break down at elevated temperatures.

Infrared thermography

Infrared thermography can provides spatial temperature distributions as opposed to discrete radiometer measurements. This technique has been used in-flight to measure transition on a ventral fin mounted on the centreline store station on an F-15B at Mach 2 (Banks *et al.* 2000). The upcoming ESA Expert (European eXPERimental Reentry Testbed) flight will carry pyrometers to measure the temperature history on the backside of the C/C-SiC nosecone and a near-infrared camera to measure the transient temperature distribution on the inner surface of one of the four open flaps located at the rear end of the vehicle (Del Vecchio *et al.* 2009). The heavily instrumented Expert capsule will descend from 100km at 5 km/s maintaining Mach numbers in the range 15-17 down to approximately 40km altitude. Use of infrared thermography requires the carriage and appropriate placement of a compact, robust sensor and knowledge of the emissivity distribution of the surface. It may also be prone to the influence of solar reflection if used to view external surfaces. Suitable IR sensors have been developed for missile guidance but are expensive and not readily available for university-based research. Infrared thermography has been used successfully by the HYTHIRM Project to measure the heating distribution across the thermal protection tiles on the lower surface of the Space Shuttle during reentry (Horvath *et al.* 2010). The thermographic imaging was performed using the powerful optics of the Cast Glance system aboard a US Navy P-3 surveillance aircraft.

TSPs and thermal phosphors

Phosphor-based luminescent coatings, which can be divided into organic polymer-based temperature sensitive paints (TSPs) and inorganic ceramic coatings of thermographic phosphors, have more recently found wide application in aerothermodynamic testing in wind tunnels (Allison & Gillies 1997, Liu & Sullivan 2005). These coatings luminesce at a longer wavelength when illuminated by a specific shorter wavelength of light and the intensity of this luminescence is a function of temperature. Like TLCs the polymer-based TSPs are limited in usable temperature range (~100 K to 570 K) and are thus also unsuitable for hypersonic flight tests. The application of inorganic thermographic phosphors for the measurement of surface temperatures up to 2000 K in ground-based test rigs has recently been reported (Khalid & Kontis 2008) but these coatings still require careful in-situ illumination and imaging in real-time for measurements of transient heating. While these thermographic phosphors do hold great promise for use on hypersonic flight tests their use will be necessarily restricted to limited regions that can be easily illuminated and imaged in-flight.

Permanent-change thermal paints

A common strategy in the gas-turbine industry, for the operational testing of components in equally hostile environments, is the use of thermal or temperature indicating paints (Bird *et al.* 1998, Diakunchak *et al.* 2004, Lempereur *et al.* 2008). This allows the global mapping of peak temperature distributions on components such as turbine blades and combustor cans without the complexity, cost and intrusion of traditional electrically based temperature sensors. These thermal paints were initially developed in the middle of last century for industrial testing applications⁵. They utilise special paint mixtures that undergo chemical reactions at specific temperatures that result in visible colour changes. Development of these paints has resulted in mixtures that irreversibly undergo either a single change or multiple changes in colour at a range of elevated temperatures.

Thermal paints are ideal for use in flight tests where structural temperatures are of interest. In the case of hypersonic flight tests, where the heating can be extreme, the peak temperature distributions from strategically located patches of paint could be used to validate design predictions of surface temperature. This of course requires recovery of the vehicle for post-flight inspection. While it is known by the authors that these paints have been exploited for flight-test applications, other than a discussion of the use of thermal paint to investigate the heat transfer to a pylon-mounted store on a supersonic combat aircraft (Matthews & Key 1977), the available literature is close to non-existent.

While some early use of thermal paints on X-15 flight tests has been reported (Reed & Watts 1961, Jenkins & Landis 2003), published records do not indicate that it was used to provide quantitative temperature data. The key aspect here is that the thermal behaviour of the aero-structure of a flight vehicle will often be strongly transient. There is almost no published work on the transient behaviour of these paints, particularly over the short durations of interest to experimental flight programs such as HyShot/HIFiRE where atmospheric heating typically occurs for durations shorter than 60 seconds. During such flights the "heat sink" aero-structure designs that we have tended to use are never able to thermally equilibrate.

Summary

Permanent-change thermal paints offer a number of distinct advantages for global temperature mapping on hypersonic vehicles over other established techniques (Table 1). While the accuracy of these paints does not match more traditional thermocouple arrays, they do offer many practical advantages such as reduced cost and mass and bandwidth penalties. Careful use of paint coatings, used in tandem with more accurate point measurements from thermocouples could help to build a much more detailed understanding of the complex distribution of heating across a hypersonic vehicle.

Table 1. Comparison of techniques for in-flight global temperature measurement

Method	temperature resolution	spatial resolution	temperature range	realtime illumination required	realtime observation required	telemetry bandwidth required	payload weight penalty	payload recovery required
Thermocouple arrays	high	low	high	No	No	Yes	Yes	No
Infrared thermography	high	high	high	Yes	Yes (thermographic camera)	Yes	Yes	No
coating based methods								
Thermochromic liquid crystal (TLC)	medium	high	low (<150°C)	Yes (white light)	Yes (visible)	Yes	Yes	No
Temperature Sensitive paint (TSP)	medium	high	medium (<300°C)	Yes (narrow band)	Yes (narrow band)	Yes	Yes	No
Thermal Phosphors	medium	high	high (up to 1600°C)	Yes (narrow band)	Yes (narrow band)	Yes	Yes	No
Permanent-change thermal paints	low	high	high (>1300 °C)	No	No	No	No	Yes

Calibration Strategies

A number of calibration strategies are under development to quantitatively interpret the response of the permanent-change thermal paint coatings on the test vehicle. As identified above, the purely qualitative response of the paints can provide insight into the relative spatial distribution of heating and allow the identification of hot spots as it did on the early X-15 flights (Reed & Watts 1961, Jenkins & Landis 2003). Ideally though a quantitative measurement of the surface temperature history is desired.

Four strategies are currently under development for using thermal paints for hypersonic flight test. In order of increasing complexity they are:

1. Qualitative use of the paints to provide accurate spatial indication of hot spots and relative heating.
2. Post-flight validation of numerical predictions of vehicle temperatures via comparison of final paint colours on the recovered vehicle with those obtained from ground-based calibrations using a reproduction of the predicted surface temperature histories.
3. Post-flight validation of numerical predictions of vehicle temperatures via comparison of final paint colours on the recovered vehicle with those predicted from knowledge of the paint chemistry and the predicted temperature histories.
4. Direct deduction of the surface temperature history from a recovered set of final paint colours via inverse methods.

All of these methods require an improved understanding of the transient response of the paints under high heating loads and thus a method for reproducing these heating histories on the ground.

Transient Heating Calibration Rig

In order to experimentally represent surface-heating profiles such as those experienced by hypersonic re-entry vehicles and consequently test the transient response of thermal paints, a simulation method must be implemented that achieves a large increase in heating rate over a short period of time.

Oxy-acetylene torch heating

Neely and Tjong (2008) established the use of an oxy-acetylene torch to heat the back surface of thin steel test plates coated with thermal paint. Constricting the flame impingement to a small circular area through the use of an insulating brick with a 16mm hole placed between the test piece and the torch ensures consistency of heating. By traversing the oxy-acetylene torch towards the sample, an exponential time-temperature profile was obtained similar to that experienced by hypersonic re-entry vehicles. Both an infra-red thermographic camera and a CCD camera were used to simultaneously record the visible colour change and the surface temperature of the test pieces, and these sequences were analysed to obtain the time-temperature-colour response of the paint at various locations on the sample (Figure 1).

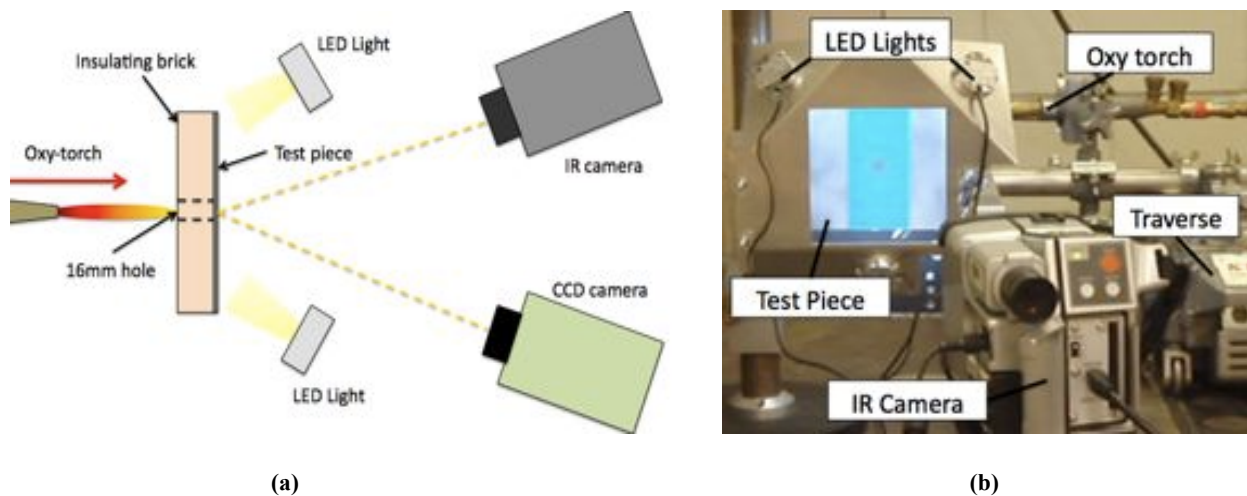


Figure 1. (a) Schematic and (b) photograph of oxy-acetylene torch transient calibration setup showing the painted test plate, insulating brick, IR and CCD cameras and LED lights.

We have evolved this method to obtain data at a range of heating rates from a single test. The transient calibration induces a range of temperature-time histories at different radial positions from the centre of the flame impingement on the rear surface of the test plate. The dependence of colour response on heating history means that calibration data must be obtained for a variety of heating rates. Figure 2 shows an IR camera image of the heated plate with the corresponding temperature of the painted surface as a function of time for various locations on the sample. It can be seen that the temperature profile increases exponentially at a range of heating rates.

The CCD and IR camera sequences are synchronised to obtain colour and temperature histories for each point on the surface. Uniform lighting conditions have been achieved through the use of three white LED cluster lights placed around the test sample at 120° apart (Figure 1b). The lights used were commercially available 7-LED clusters. It was found that the strength of the LED lights was sufficient to eliminate the effect of background lighting on the colour data produced from the digital processing of the CCD images. LEDs were selected over other light sources to minimise radiative heating of the test samples but their use may have to be reassessed if their spectra are found to be too nonuniform.

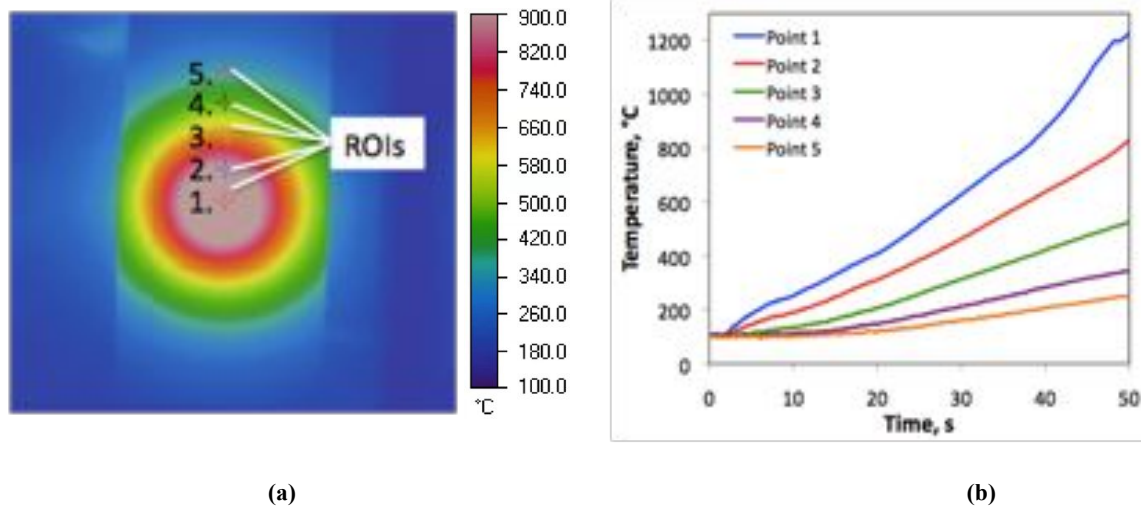


Figure 2. (a) Still image from IR camera history of transient calibration test showing regions of interest (ROIs) with (b) matching surface temperature histories at various radial locations outwards from the centre of heating.

The CCD images are subsequently processed using a MATLAB routine to extract the hue, saturation and brightness/value (HSV) values of the colour for groups of pixels at a range of points on the painted surface (Figure 3). This colour data is matched with the corresponding temperature at each point for all images in the sequence. To reduce noise, square groups of nine pixels around each point are analysed and the colour values were averaged to provide a single colour value at the location of the centre pixel. Figure 3c shows example HSV colour data as a function of temperature and time for the centre point of a sample painted with the single-change thermal paint SC275, which is designed to transition from blue to cream at 275°C.

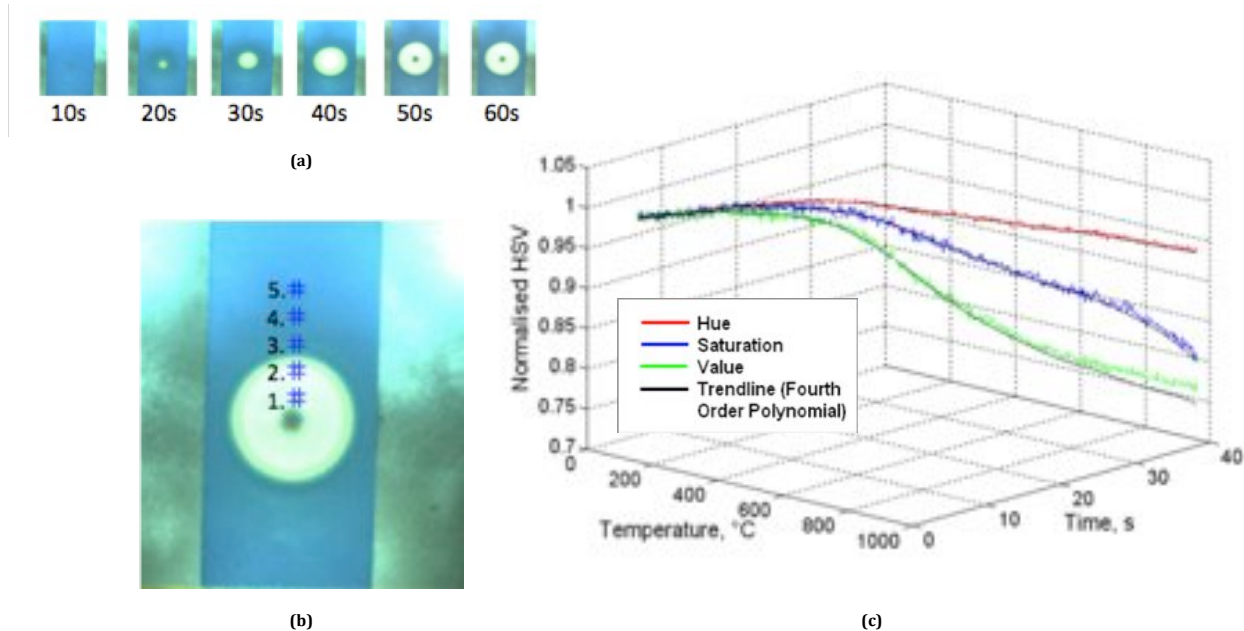


Figure 3. (a) Colour change for SC275 thermal paint during transient heating with oxy-acetylene torch. (b) Data collection regions. (c) Histories of HSV and temperature data for region 1.

It can be seen that hue changes very little throughout the colour transition, while changes in saturation and value are more apparent. HSV values are of pertinent because of their approximate correlation with visible spectral data (Padgham & Saunders 1975) and these can be calculated as a function of both temperature and time for any point on

the sample. This procedure can be repeated for a range of paints, and in this manner, colour-change datasets are compiled for various heating rates for each paint.

The oxy-acetylene torch has now been replaced with an electric-arc heater to provide the transient heating to enable accurate non-linear control of the heating rate to allow simulation of any surface temperature history of interest. This will provide the calibration data required for methods 2 and 4 listed in the previous section.

Electrical resistance heating

Another calibration method that is suited to varying surface temperatures is resistive heating. A voltage difference is applied across an electrically conducting painted coupon. The resistive power dissipated in the coupon is a function of the electrical resistance of the coupon and the voltage applied. This technique has been favoured by Rolls-Royce for calibration of thermal paints applied to gas turbine (Nash & Dempster 2005). To maximize the temperature rise for a given electrical power the resistivity of the sample should be high, but the material must also retain its electrical and mechanical properties at high temperatures. Kanthal-AF, a commercial alloy of iron, chromium aluminium and cobalt is frequently employed as a heating element. It has a higher resistivity than Nichrome a higher maximum temperature capability and is thus well suited for this application.

To maximize the resistive heating the cross section of the test piece can be reduced. This is achieved by both reducing the thickness of the plate and by tapering its width down to a neck thus forming a bow-tie arrangement (Figure 5) a technique that has been employed in industrial calibrations (Nash & Dempster 2005). This tapering also serves to induce a steep gradient in temperature toward the narrowest point, which produces a range of calibration data across the coupon in a single time point of a calibration test. It was found that a minimum thickness of 1 mm was sufficient to resist distortion at the temperatures reached in these initial tests.

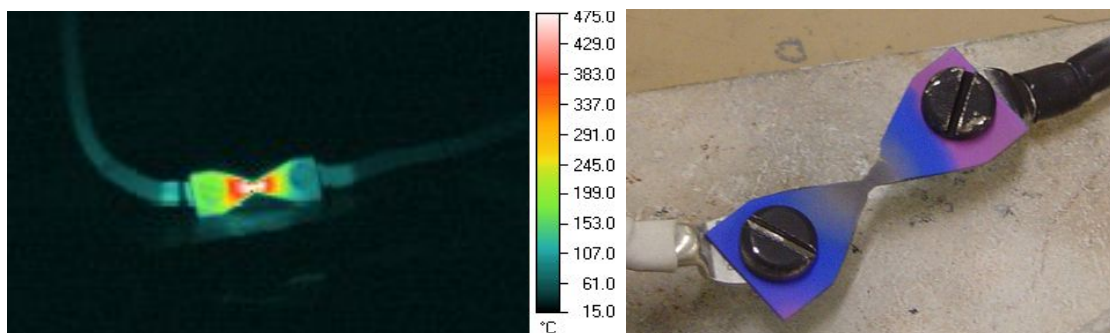


Figure 4. (a) Thermal image of the thin bow tie and power supply cables. The painted coupon reached a maximum of 505°C, (b) post-heating distribution of paint colour (MC165-2) on the coupon after the calibration.

One or both sides of the heating element can be coated with thermal paint and viewed by the IR camera and the colour video camera. For these initial tests the current was supplied by a 1 kW DC power supply. For this trial the power was ramped up manually but for accurate calibrations of flight heating this power supply could be computer controlled to induce a specified surface temperature history on the painted sample. The rapid surface temperature increase that can be induced by this technique is apparent from the heating histories shown in Figure 5, although the peak temperature achieved is limited by the output of the power supply. The resultant colour transitions of a multi-change paint (MC165-2) are apparent in the figure to be emanating from the neck of the test coupon where the temperature rise was maximum.

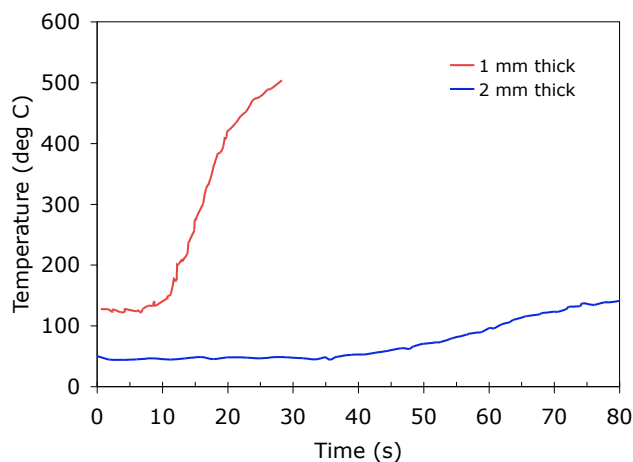


Figure 5. Temperature history for resistive heating of painted KANTHAL-AF bow-tie samples of different thicknesses.

Laser-based radiative heating

Another method to heat the painted sample during calibration is to do so radiatively. This was attempted in initial calibration trials (Neely & Tracy 2006) using a high temperature oven in which the heat transfer mode was primarily radiative from the oven walls though there was also a component of free convective heat flux from the heated air in the oven. While ovens are used in industry for calibration of thermal paints over longer durations at nominally steady soak temperatures this technique was shown to not be suitable for application to short duration flight tests. This was because of the extended soak times required even at high temperatures to heat the samples and the decreasing rate of heat flux experienced by the calibration sample as it increased in temperature due to the decreasing temperature difference. While ramping of oven temperatures is possible via a controller, it is typically too slow to mitigate this drawback over the short durations required.

An alternative method is to use a high-powered continuous-wave (CW) laser to illuminate an area of the surface of the painted sample (Figure 6). Calculations show that a 100W CW CO₂ laser would be just suitable to illuminate a small 4 mm diameter spot and produce the heat flux necessary to induce the required changes in surface temperature. The heat flux to the sample could be ramped up by either translating the sample toward the laser or by reducing an initial masking of the impinging beam. One advantage of this technique is the ability to directly measure the rate of energy input to the surface via a laser power meter. Additionally, like the oxy-acetylene torch, laser heating does not require an electrically conducting target material and could thus be applied to non metallic substrates such as ceramics that may well be of interest for use on thermal protection systems, fins or even combustion chambers on hypersonic vehicles.

This technique, while being potentially well suited to the problem, has not yet been attempted by the authors. Originally it was intended to acquire an appropriate 100W CW CO₂ laser but even the power of this laser was marginal, especially if absorption of all of the laser energy could not be guaranteed. Additionally new OH&S restrictions on the use of Class 4 (Australian rating) laser products at UNSW@ADFA makes the use of such a laser almost impractical in our laboratories. Even though a laser-based heating rig had been designed and budgeted these constraints forced the investigation of an alternative method of delivering large amounts of energy to the test sample, quickly and controllably and this is being developed using electric-arc heating.

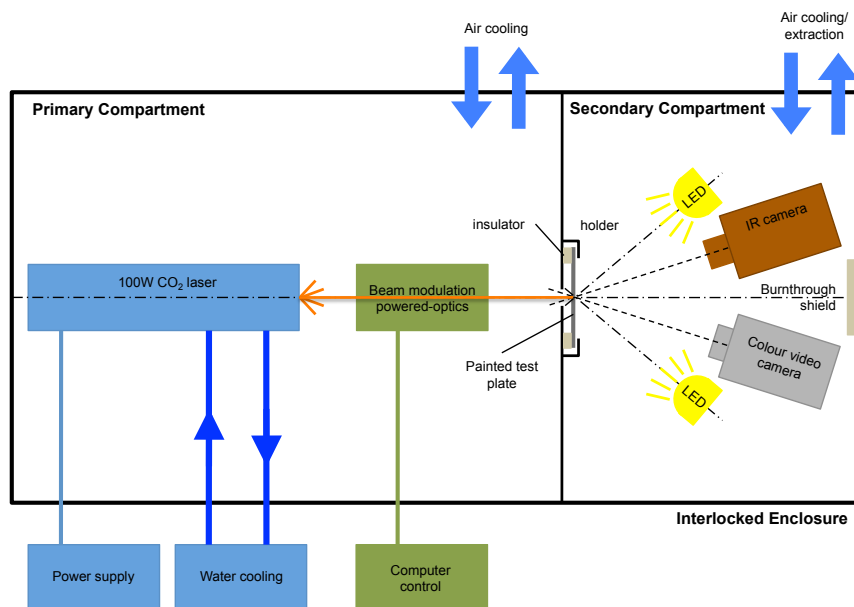


Figure 6. Radiative heating using a CO₂ laser illuminating either the front or rear surface of the painted sample.

Electric-arc based heating

A large industrial TIG welder (Miller Dynasty 350) has been acquired to power the transient heating calibration rig for the paints. This welder is capable of a peak power output of 16kW (rating 300 A at 32 V, 60% Duty Cycle) which is well beyond the requirements of much of the calibration testing and two orders of magnitude more than the equivalently priced industrial CO₂ laser could deliver. The welder generates a plasma arc, which is used to heat the sample from the rear side (Figure 7). This requires the grounding of the sample, which is not an issue for the direct heating of a metal sample but requires a different solution for non-metallic samples.

This is achieved by the use of an electrically-conductive target heat sink which is connected to the circuit of the welder (Figure 8). This target piece can also be used to spread the thermal footprint of the input energy across the painted sample piece. Initial tests have been performed with cylindrical copper target pieces to assess the effectiveness of this technique. Ongoing numerical and experimental work is investigating the use of contoured target pieces to efficiently spread the heat input without the penalty of a large thermal mass in the heat sink. With the addition of the target heat sink the electric-arc heating technique can be applied to non-metallic test samples such as ceramic or ceramic-based composites.

The heat sink can also be used for high temperature experiments recreating extreme heating conditions in which the power of the electric arc impinging on the sample plate can erode the sample. Instead a tungsten or sacrificial steel heat sink can be used to either avoid any erosion or at least to restrict it to the heat sink.

The use of the target heat sink relies on good thermal conduction between the heat sink and the painted sample. Testing has shown that this can be adequate for two flat metal surfaces but the thermal contact can potentially deteriorate if the painted sample, which is usually a thin plate, thermally distorts. Experimental trials are being undertaken using a commercial high temperature heat conducting paste (Thermon® T-99) rated up to 1000 °C to ensure a good thermal bond between the target heat sink and the sample. Additionally the paste is electrically non conductive. While the paste is designed to set and provide a permanent bond, the long curing time allows the paste to be applied and used for these short duration tests and then be removed before it sets. Trials using the paste will be reported in a later addendum.

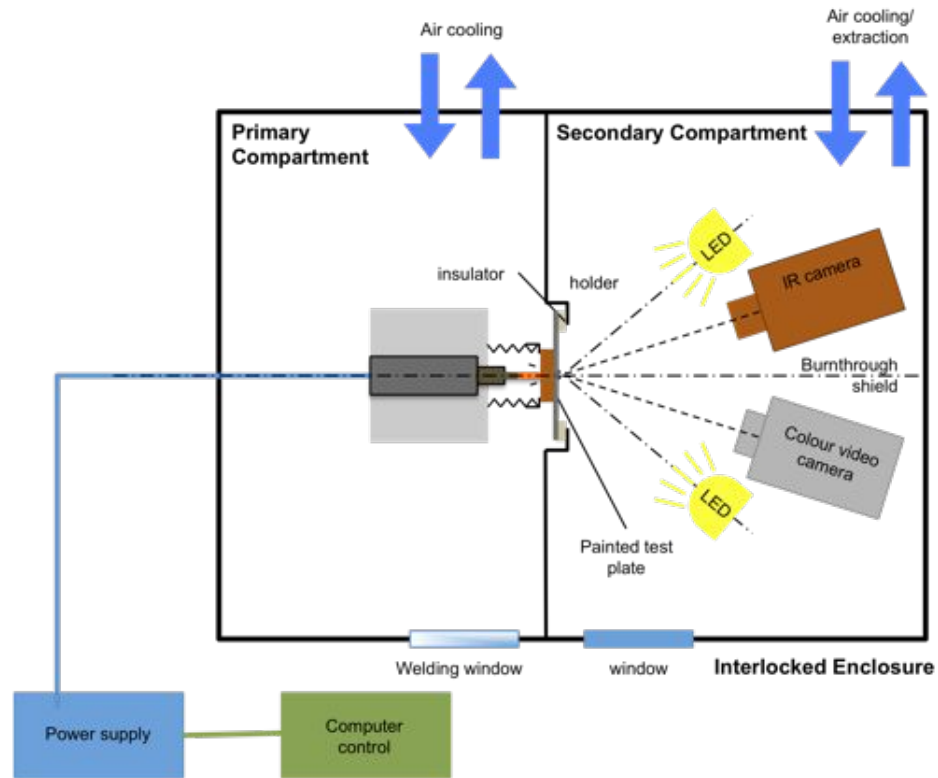


Figure 7. Schematic of electric-arc based calibration rig

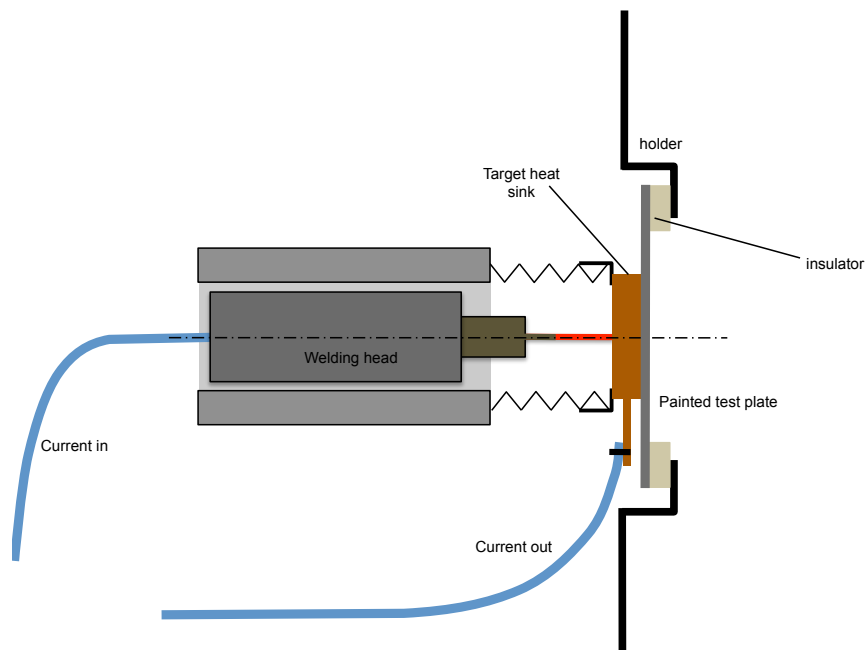


Figure 8. Detail of sample mounting with the addition of a target heat sink

A range of cylindrical copper target heat sinks were manufactured to investigate the thermal contact between the heat sink and the sample plate and the resulting heat spreading. Six copper cylinders of diameters 20 and 25 mm and depths of 2.5, 5, 7.5 and 10 mm were tested on a horizontal sample plate, viewed from beneath. This orientation was chosen to use the weight of the copper target to ensure good thermal contact. In the final rig, with the sample plate held vertically, this thermal contact will be improved by the use of positive spring force (Figure 8).

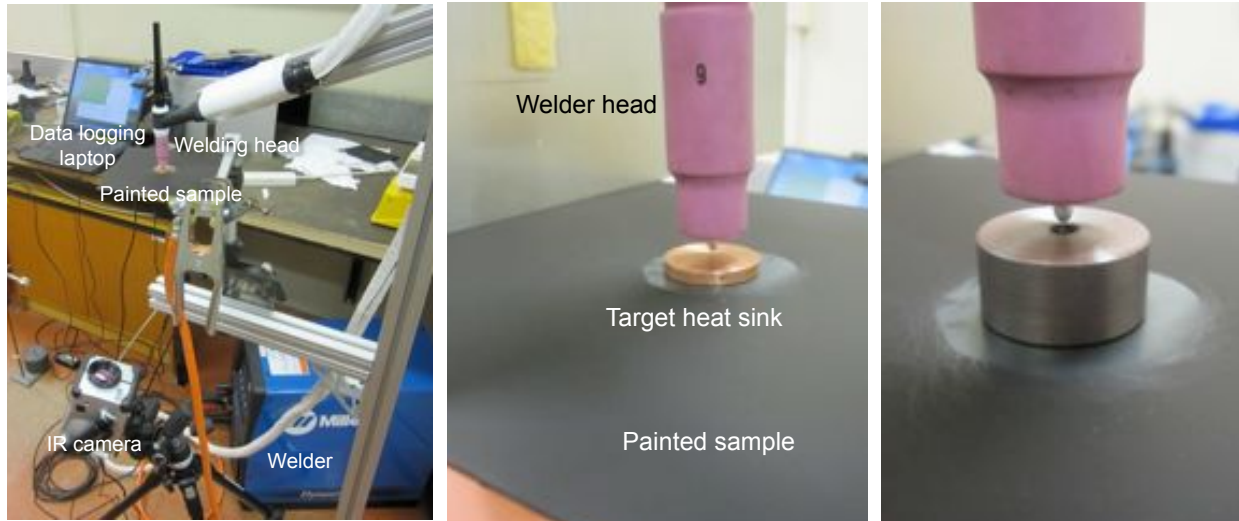


Figure 9. Testing of the target heat sinks (a) experimental lay out, close up of the (b) 2mm thick and (c) 10 mm thick copper target heat sinks centrally located on the mild steel sample plates.

FEM simulations were performed for a range of target heat sink diameters, depths and materials (Figure 10). Increasing the diameter and depth of the heat sink increased the thermal spread as it increased the lateral conduction path radially out along the plate. Increasing the thermal mass in this way also decreased the peak temperature and lengthened the temperature rise time on the front of the plate. Thus a compromise is required between enough thermal spread and too much thermal mass. Figure 11 shows infrared thermographs of the plate viewed from below, with and without a target heat sink in place. It can be seen that the heat sink works as expected, increasing the spread of heat but decreasing the peak temperature.

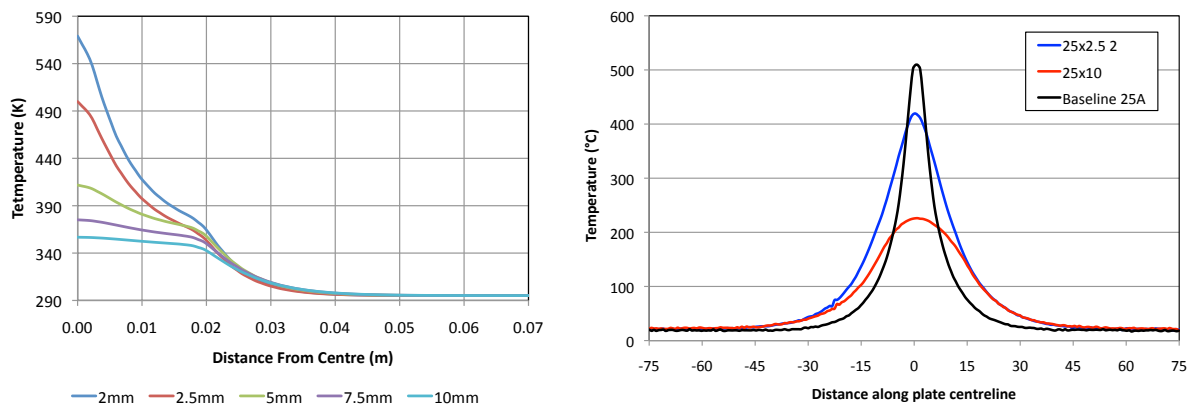


Figure 10. Comparison of (a) FEM predictions of radial temperature distribution across the backside of the sample plate in perfect thermal contact with a range of cylindrical copper target heat sinks with (b) experimental measurement of the temperature distributions for a higher power setting.

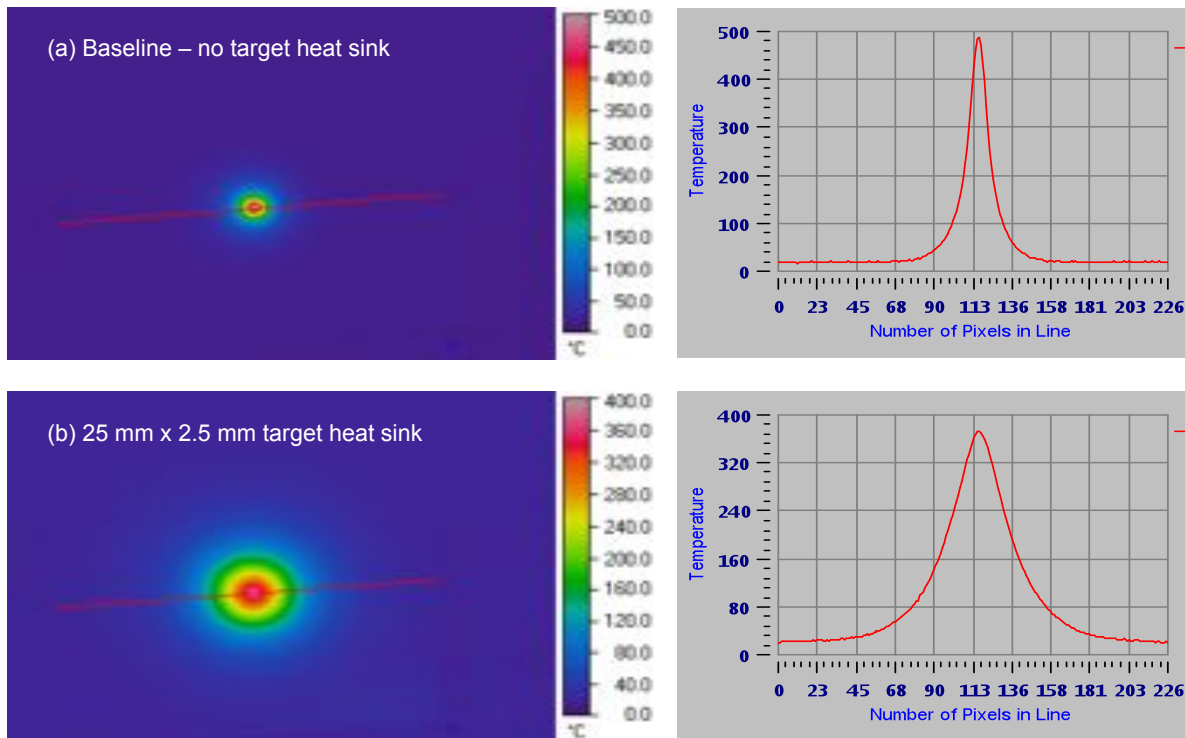


Figure 11. Infrared thermograms and temperature distributions across the 150x150x1.6 mm mild steel plate (a) with no target heat sink and (b) with a 25 mm diameter x 2.5 mm deep copper target heat sink. The red region-of-interest line

The advantages of the electric-arc based heating are that the welder is able to supply sufficient power to induce flight representative temperature changes on the painted surface of the samples and that the power input via the arc can be easily computer controlled to simulate desired heating histories for different locations on a vehicle and different trajectories. Additionally, through the use of the target heat sink, improved thermal spreading is achieved and the heating technique can be applied to a range of non-metallic materials.

Data capture during transient heating experiments

As well as providing the end-state colour of the paints after exposure to a defined temperature history, the heating rig allows the measurement of the transient colour change. The rig incorporates an IR thermographic camera and CCD camera to record both the surface temperature and surface colour distribution histories during the heating. In addition a fibre-optic spectrometer is used to record the changing spectra at a point on the sample during the test. This provides significantly more data than the CCD camera to assess the transient of the colour change. Initial testing has been performed using an AvaSpec UV-2048 optical-fibre spectrometer and example spectra from this instrument captured during transient heating on the oxy-torch rig are shown in Figure 12. As this spectrometer was limited to wavelengths above 480 nm it has since been replaced with an equivalent AvaSpec UV-2048 with increased spectral coverage of 350 to 870 nm. This spectrometer will be used on future transient calibration experiments on the electric-arc heating rig.

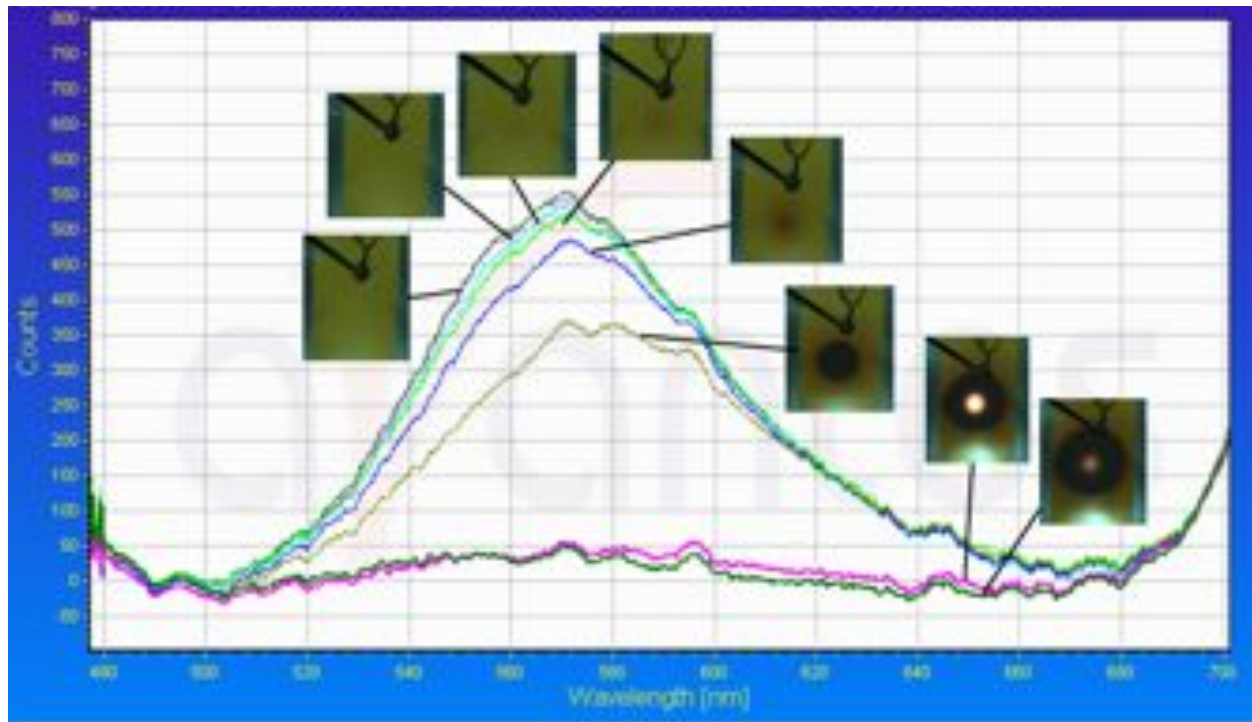


Figure 12. Fibre-optic visible spectrometer measurements of colour transition during transient heating of painted sample.

Chemistry of the Permanent-Change Thermal Paints

As discussed, the transient response of permanent-change thermal paints is not properly understood. In particular the final colour of the paint is a function of the temperature history and not just the maximum temperature of the surface to which they are applied (Kafka *et al.* 1965, Neely & Tracy 2006) (Figure 13, Figure 14). We are working to establish the dependence of the chemical behaviour on the history of thermal input to the paint coating using controlled heating and spectroscopic measurements of the paint response for a series of commercially available single-change (SC) and multi-change (MC) paints.

As the visible colour of the painted surfaces is a function of the molecular structure of the thermal paints and the permanent colour changes are a result of endothermic reactions, for calibration method 3 listed above, it is required to accurately characterise the paint chemistry. This is necessary to determine the pre-exponential factor and the activation energy in the Arrhenius equation and thus define the temperature dependence of the reaction rate of each molecular change and thus colour change for a given paint (Neely & Tjong 2008)

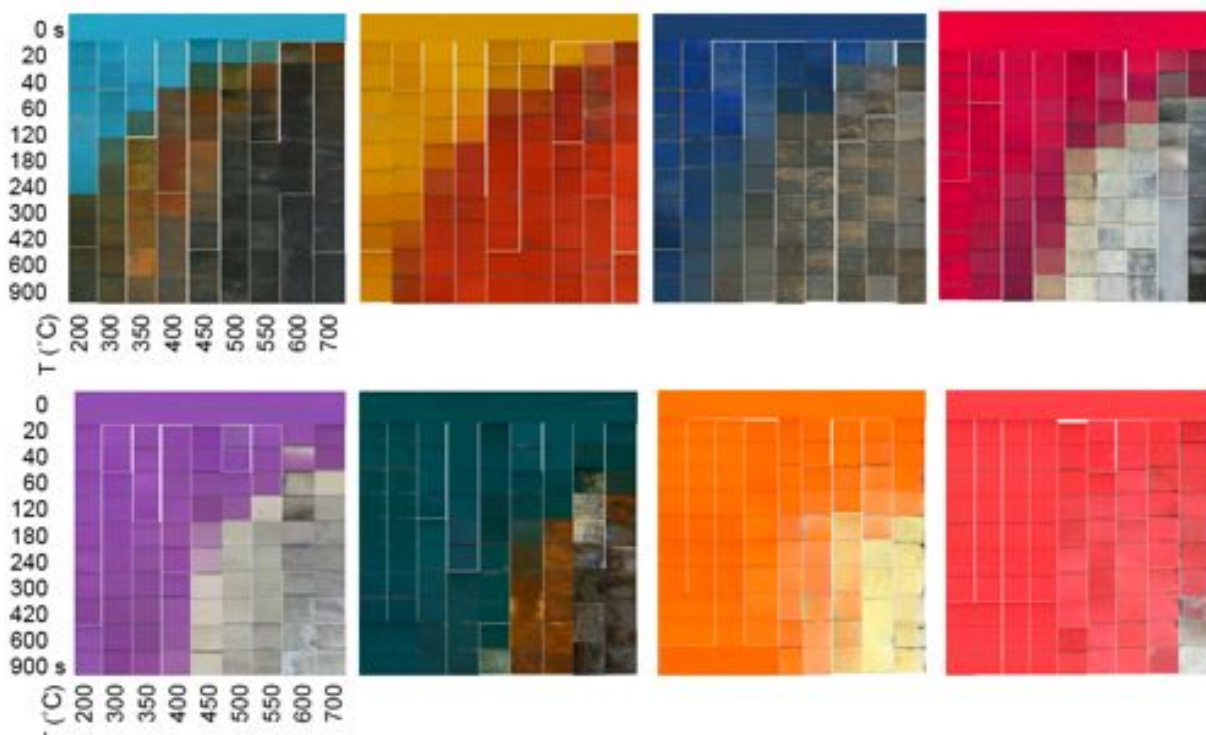


Figure 13. Calibration colour maps for the single-change paints: SC155, SC240, SC275, SC367, SC400, SC458, SC550, SC630. (Neely & Tracy 2006) Note that this digital images have not been colour corrected.

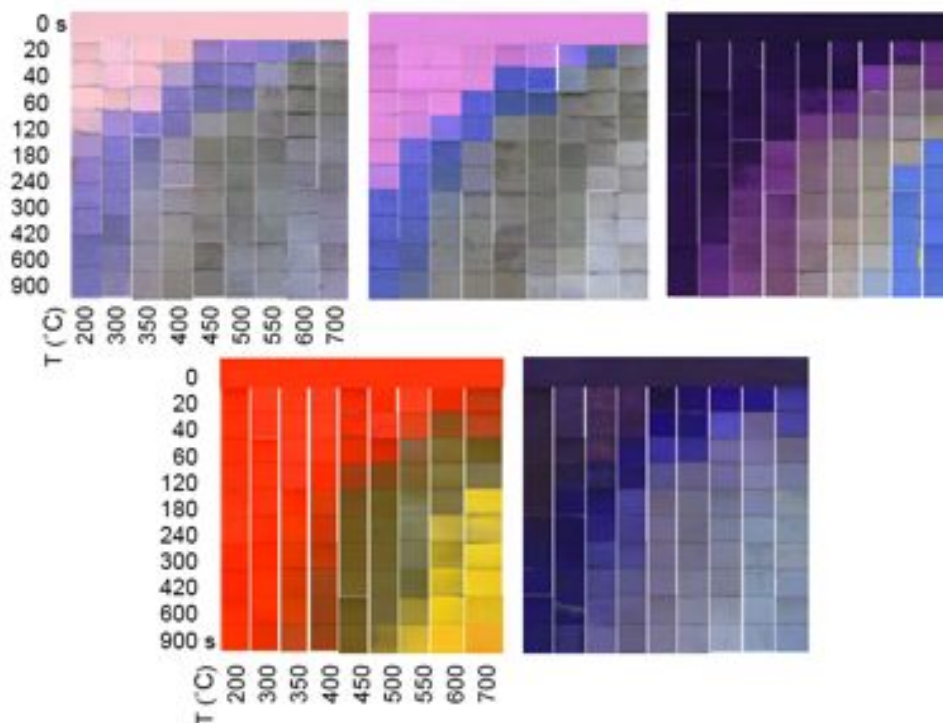


Figure 14. Calibration colour maps for the multi-change paints: MC135-2, MC165-2, MC395-3, MC490-10, MC520-7.
(Neely & Tracy 2006) Note that this digital images have not been colour corrected.

Elemental analysis of paints using X-ray fluorescence

Although the manufacturer of the Thermax® permanent-change thermal paints (TMC-Hallcrest) provides specification sheets and a full MSDS listing some of the components, the actual mixture is not provided. We have used X-ray fluorescence to establish the chemical makeup of the paints.

Elemental analysis is commonly performed using X-ray spectroscopy, which exposes a test sample to high-energy X-rays. The molecules in the sample absorb this X-ray radiation and electrons in lower orbitals are excited from their ground state to a higher state. The electrons from the higher energy outer shells fall into these lower orbitals, releasing energy equivalent to the electrical difference between the two orbitals (Tertian 1987). This energy is re-emitted as fluorescent X-rays and the amount of energy is characteristic of the atomic source. This type of spectroscopy is typically able to detect heavy elements, making it especially suitable for identifying metallic compounds, such as those found in the permanent-change thermal paints.

PVC coupons were painted with a sample of each of the paints and excited with x-rays in an x-ray fluorescence spectrometer. The PVC substrate was used to avoid contaminating the measurements, as the lighter plastic hydrocarbon molecules will not be detected by the spectrometer. The spectrometer recorded the resulting x-ray fluorescence from the paints revealing the chemical make up. These measurements also served to establish which paints had suitable chemistry for monitoring via IR transmission spectroscopy.

Example spectra are shown in Figure 15 for a single-change paint (SC275) and a multi-change paint (MC490-10). The presence of particular metallic compounds is apparent from the spectra, for example the titanium in the SC275. The -K α and -K β suffixes denote the level of atomic orbital responsible for the release of energy. The increased number of components is visible in the spectra for the multi-change paint (MC490-10)

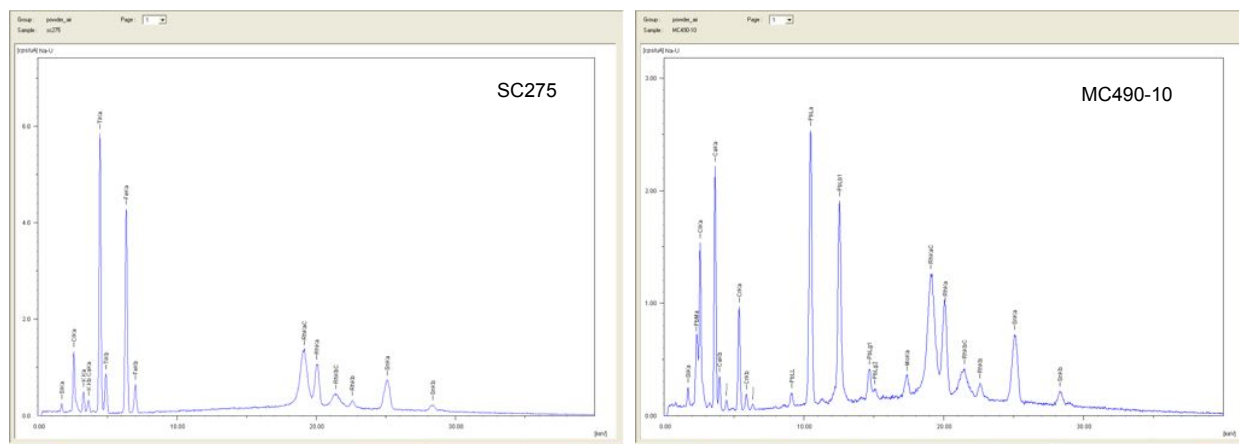


Figure 15. Example x-ray fluorescence spectra for (a) SC275 and (b) MC490-10

Monitoring chemical changes via IR transmission spectroscopy

An IR transmission spectrometer is being used to determine the chemical compounds present in the thermal paint through identification of characteristic IR absorbances of different chemical bonds. IR wavelengths are able to detect covalent bonds and can therefore detect the emission of organic molecules from the metallic atoms within the coordination complex. Small, clear potassium bromide (KBr) disks are coated with a thermal paint and the sample was placed in the IR spectrometer at different stages of the colour transition induced by previous heating of the sample. The KBr disks are largely transparent to IR radiation. The colour transition, and hence the chemical reaction that causes it, is a function of both temperature and time. The chemical reaction requires a given activation energy, and the probability of any given molecule reaching this energy and undergoing a chemical change increases with temperature.

Two methods of measuring different stages of the chemical reaction have been explored. In the first, paints are heated at a range of temperatures for a given period of time. Temperatures spanning the manufacturer-specified transition in small increments are used and the colour change at each temperature is observed. The second method is to heat the samples coated with a particular paint at the same temperature for different time periods.

An example of this second method, applied to the spectral analysis of SC155 using the IR transmission spectrometer, is shown in Figure 16. The chosen temperature for these measurements was the transition temperature indicated by the manufacturer (155°C). The paint was heated at two-minute intervals and the IR spectrum was measured after each time period. Figure 16 shows the IR spectrum of SC155 at each time step, and it can be seen that several noticeable changes occur within the molecular bonds as the colour transition progresses. IR correlation tables given by George and McIntyre (1987) were used to identify the absorbance peaks (given by depressions in the transmittance spectrum). It is known that several of the thermal paints emit phosphorous upon heating, and this can be seen in the change in peak absorbance of the P-H bond at each time interval. The un-heated sample shows a large absorbance band indicating O-H bonds and this is likely to represent water molecules, which simply evaporate on heating and do not contribute to the chemical reaction within the paint.

IR spectroscopy is almost completely limited to the identification of covalent bonds. While this is useful when applied to thermal paint chemistry in identifying the release of ammonia, phosphate, and carbon-dioxide molecules that occur during the chemical reaction, it is assumed that the colour change is a result of the dissociation and recombination of metallic salts (Cowling et al. 1953). These bonds are ionic and therefore cannot be identified through IR spectroscopy, which also explains the small degree of change in transmittance bands in Figure 16.

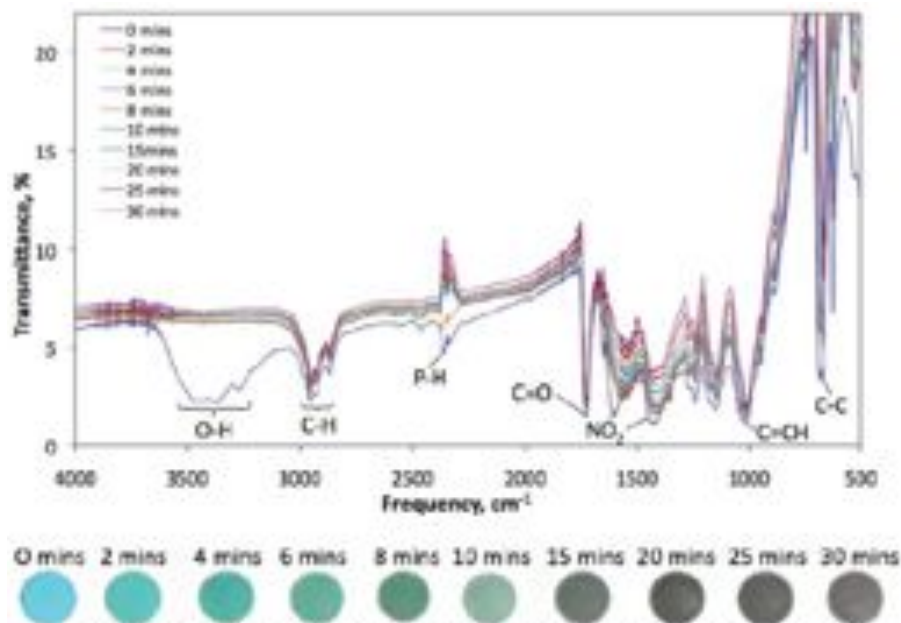


Figure 16. IR transmission spectra measured for SC155 after heating at 155 °C for a range of times.

Spectrophotometer measurements

As the visible colour of the painted surfaces is a function of the molecular structure of the thermal paints and the permanent colour changes are a result of endothermic reactions, for calibration method 3 listed above, it is required to accurately characterise the paint chemistry. This is necessary to determine the pre-exponential factor and the activation energy in the Arrhenius equation and thus define the temperature dependence of the reaction rate of each molecular change and thus colour change for a given paint (Neely & Tjong 2008).

A UV/visible spectrophotometer is being used to provide a spectral analysis of each paint as it is able to simultaneously measure both the absorbance and reflectance bands of a coloured surface. However, the use of this device is limited as a small sample must be inserted into the spectrophotometer where measurements are taken internally and therefore it cannot be used to measure the dynamic response of the thermal paints. An AvaSpec UV-2048 optical-fibre spectrometer is therefore being used in tandem to acquire spectral information from the transient tests.

Colour analysis using the spectrophotometer is being performed using samples exposed to well defined long-duration heating. These samples are oven heated to provide colour data for the steady-state response of the paints. It was found that the minimum 10-minute heating time recommended by the paint manufacturer was insufficient to reach a steady state surface colour and samples were therefore heated for 30-minute periods. The samples were progressively heated at fixed intervals, with each sample representing the long-duration colour response for a given temperature. It was found that for all paints tested, the colour change began to occur at lower temperatures than indicated by the manufacturer.

Figure 17 shows oven-heated samples of the single change paint SC155 and the reflectance spectrum for each temperature. The percentage reflectance at the dominant wavelength begins to decrease as the colour-change reaction has progressed for this paint from blue/green to dark brown.

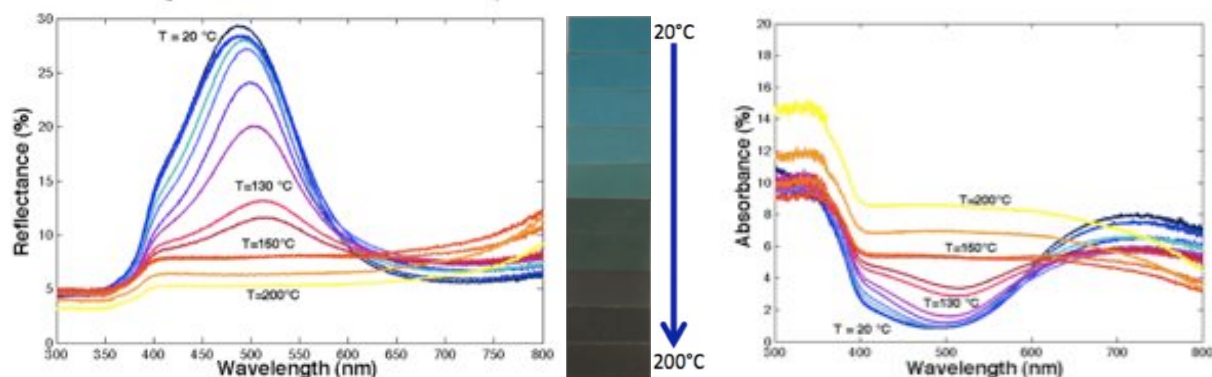


Figure 17. Measurements of colour response of SC155 samples exposed to oven heating from 20°C to 200°C using spectrophotometer. (a) Reflectance spectra and (b) absorbance spectra.

While the spectra clearly illustrate the colour change and provide a large amount of information for each colour transition, it is the absorbance of light by the surface that is directly proportional to the concentration of a given chemical species (Skoog *et al.* 2006). Changes in the absorbance spectrum indicate that a chemical reaction, and hence a colour change, has occurred. The absorbance band may therefore be used to indicate how far the colour has transitioned by measuring the level of completion of the chemical reaction. The matching absorbance spectra for SC155 are also shown in Figure 17 illustrating the increased absorbance of the blue/green wavelengths as the paint chemically transitions.

Figure 18 presents this absorbance data at different wavelengths as a function of temperature. At the dominant wavelength (approximately 500 nm) it can be seen that there is no change in the absorbance and thus chemical composition of the paint until it has been heated above 100 °C. Above this temperature a dramatic increase in the absorbance is observed, indicating that a chemical reaction is occurring. While the most dramatic change is centred around 150°C, which corresponds to a distinct change in colour from green to brown and represents the nominal change point of the paint, it can also be seen that the reaction has not reached completion at the upper temperature at which data was collected. Completion would be indicated by a return to a constant, though higher, absorbance.

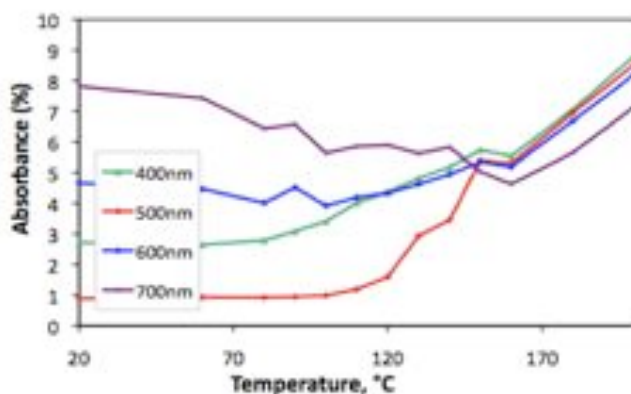


Figure 18. Absorbance vs. temperature of SC155 for various wavelengths from 400nm to 700nm.

Despite the limitations of the spectrophotometer, for paints that feature colour transitions where the dominant wavelength is easy to calculate, such as blue, green, red and yellow, the spectrophotometer is a particularly useful tool in quantifying colour-change data. It also provides a controlled and calibrated environment in which colour measurements are taken, thus reducing the uncertainty in the measurements. These spectrophotometer measurements

are being used to quantify the dependence of the chemical reaction on heat input using the Arrhenius equation. More complete results from these measurements will be reported in a later addendum.

Limitations of spectral analysis

Spectral analysis can be an extremely accurate and reliable method of quantifying colour change and it is able to provide an enormous amount of information on each colour compared to what can be obtained from a CCD. Despite these advantages, spectral analysis has several limitations. Devices that do not take measurements in a fully controlled and enclosed environment are sensitive to changes in lighting conditions that may significantly alter results. This is also a limitation in digital image analysis and may be overcome through the use of uniform lighting conditions, however such conditions are difficult to maintain and measure. Furthermore, it is difficult to measure the transient colour response using such instruments as they lack portability and restrictions on sample size limit the ability to measure the dynamic colour response under high-intensity heating.

Pressure dependence of paint response

Early development of thermal paints noted a non-ideal dependence of the colour change on the ambient pressure (Jones & Hunt 1964). This was put down to the change (presumably an increase) in the liberation of the water vapour, carbon dioxide, or ammonia ligands from the paint pigments with decreasing ambient pressure, resulting in a non-thermal colour change. This pressure dependence was reduced in subsequent paint mixtures but not entirely removed. Bird *et al.* 1998 also noted that even the newer thermal paint mixtures are affected by pressure and gas composition, and in particular by combustion gases. This may be an issue if paints are to be applied within scramjet combustors or down stream of the combustor. While the pressure dependence is obviously a potential an issue for the high-pressure environments within gas turbine combustors and turbine stages, it must also be considered for the high altitude ambient conditions experienced by a hypersonic vehicle. In fact ascending and descending vehicles will pass through a range of low ambient densities and thus the conditions around parts of the vehicle will be at pressures below 1 atmosphere.

It is therefore necessary to determine the pressure dependence of any paints to be used in flight. To this end a set of experiments were performed to examine and if possible quantify this dependence. Small mild steel strips were coated with thermal paints and heated in an enclosed gas cell placed within a tube furnace (Figure 19). Initial testing established the uniformity of temperature along the full length of the painted samples. Tests were performed using a number of paints selected to overlap in transition temperature. The paints selected for these initial tests were MC490-10 and MC520-7. The two paints were applied to opposite sides of each sample. The samples were heated in the tube furnace from ambient temperature up to 700 °C and held at this temperature for 600 seconds. These tests were performed on the painted samples at pressures of 1 atmosphere (in which the gas cell was left open) and 0.75, 0.5, and 0.002 atmospheres by reducing the pressure inside the gas cell with a vacuum pump. As the temperature within the gas cell was raised, the internal pressure of the gas cell was maintained by manual bleed to the vacuum pump.

Both paints on all of the samples were all observed to experience colour change although a degree of unexplained charring appeared to occur. The paint samples are illustrated in Figure 20 with comparison to two unheated samples of the paints used. The spectra of the paints on the samples were measured in the range 350 to 870 nm using an Avantes AvaSpec 2048 fibre optic spectrometer and are compared with the spectra for the unheated samples in Figure 20. A white LED illumination source was used for these initial measurements although this is not ideal.

The data from these initial experiments is inconclusive and the investigation of the influence of pressure on colour change is being continued. The reason for the paint charring in the tube furnace is being investigated. More conclusive results will be reported in an addendum.

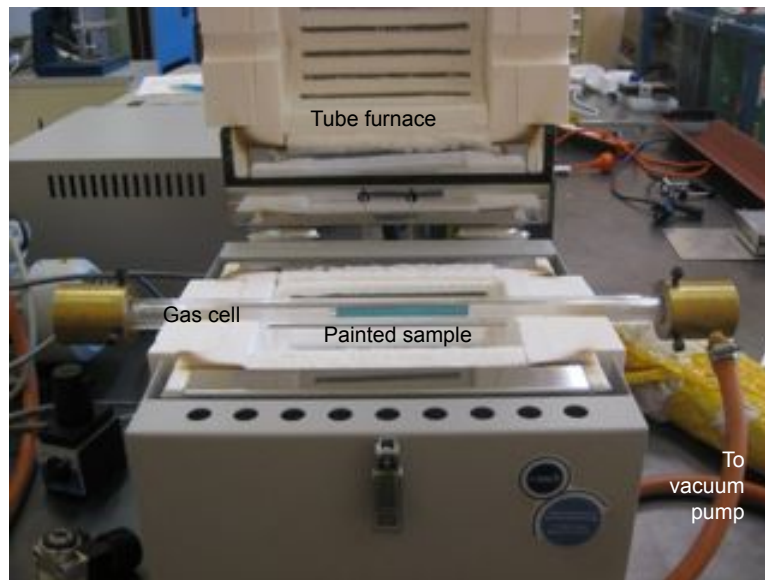


Figure 19. Pressure testing of thermal paint response.

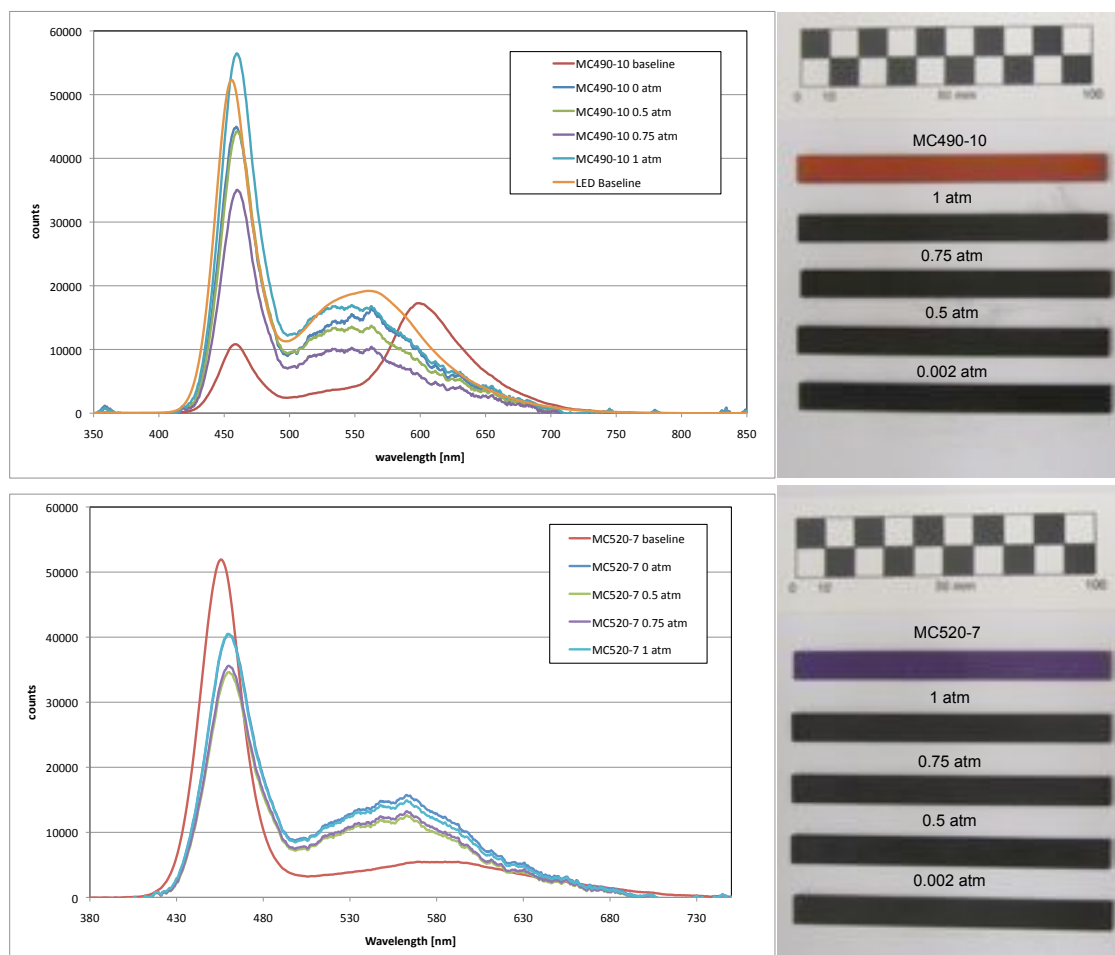


Figure 20. Before and after colour comparison of the pressure test samples: (a) spectra of samples (b) samples.

Thermal Modelling of Trajectory Heating

Efficient thermal-structural design is paramount to ensuring the performance of any hypersonic vehicle. This requires the accurate estimation of the vehicle heating across the flight trajectory and the careful design of the structure via the analysis of its response to this heating.

Initial strategies have used either analytical predictions of the heating on simplified analogs of the local vehicle geometry or steady-state CFD predictions at specific time points in the flight to provide the convective heat flux distributions to the surface. In the latter case these distributions have been temporally interpolated across the trajectory (Odam *et al.* 2005, Ho & Paull 2006, Smith 2008) to provide the boundary conditions for computational thermal-structural modelling with finite element software. Leonard *et al.* 2005 describe the highly complex combination of simpler engineering codes with higher order CFD codes used to predict the transient heating during the test flights of NASA's Hyper-X vehicle. This analysis also employed a large number of discrete CFD calculations of the convective boundary conditions. While being computationally intensive for this geometrically complex vehicle, the analysis methods were in good agreement with the flight measurements, at least for the leading edge data reported.

For the present work a combination of computational fluid dynamics (CFD) and finite element analysis (FEM) is being used to model the two-directional fluid-structure interaction (FSI) between the hypersonic flow around the vehicle and the nose cone structure. Transient simulations have been performed over the segments of the vehicle's expected descent trajectory within the atmosphere to predict the distribution of surface temperature history on the nose cone resulting from atmospheric heating.

For hot structures, which most recent hypersonic test flight vehicles employ, the transient surface temperature can strongly influence the convective heating of that surface. This strongly coupled fluid-structure interaction can be easily illustrated by considering the spherical tip of the HIFiRE-0 nose cone. Tauber²⁰ expressed the stagnation point heating on a sphere at high Mach number using the simplified relation

$$\dot{q}_{w_s} = 1.83 \times 10^{-4} \left(\frac{\rho_\infty}{r_n} \right)^{0.5} V_\infty^3 \left(1 - \frac{h_w}{h_0} \right) \quad [1]$$

Thus, for a given nose radius (r_n), the convective heat flux is a function of the product of three quantities; the square root of the freestream density (ρ_∞), the cube of the freestream velocity (V_∞) and one minus the ratio of the wall enthalpy (h_w) to the total enthalpy of the flow (h_0), the latter quantity representing the driving enthalpy difference between the flow and the wall. All three of the quantities can vary in opposition at the stagnation point for the hypersonic descent of the vehicle through the atmosphere. The density increases with decreasing altitude, the velocity initially increases under gravitational acceleration and then decreases once terminal velocity has been reached while the final quantity decreases as the wall heats up.

For the 10-second descent from 50km altitude, the quantities change as set out in Figure 21. The first two quantities (ρ_∞ and V_∞) are simply a function of the trajectory while the enthalpy difference was calculated using a lumped mass model of the nose cone tip. The resultant stagnation heat flux initially increases and then after a peak it decreases slightly as the enthalpy difference is driven down due to the increasing wall temperature. Thus the convective heating is strongly coupled to the resulting surface temperature.

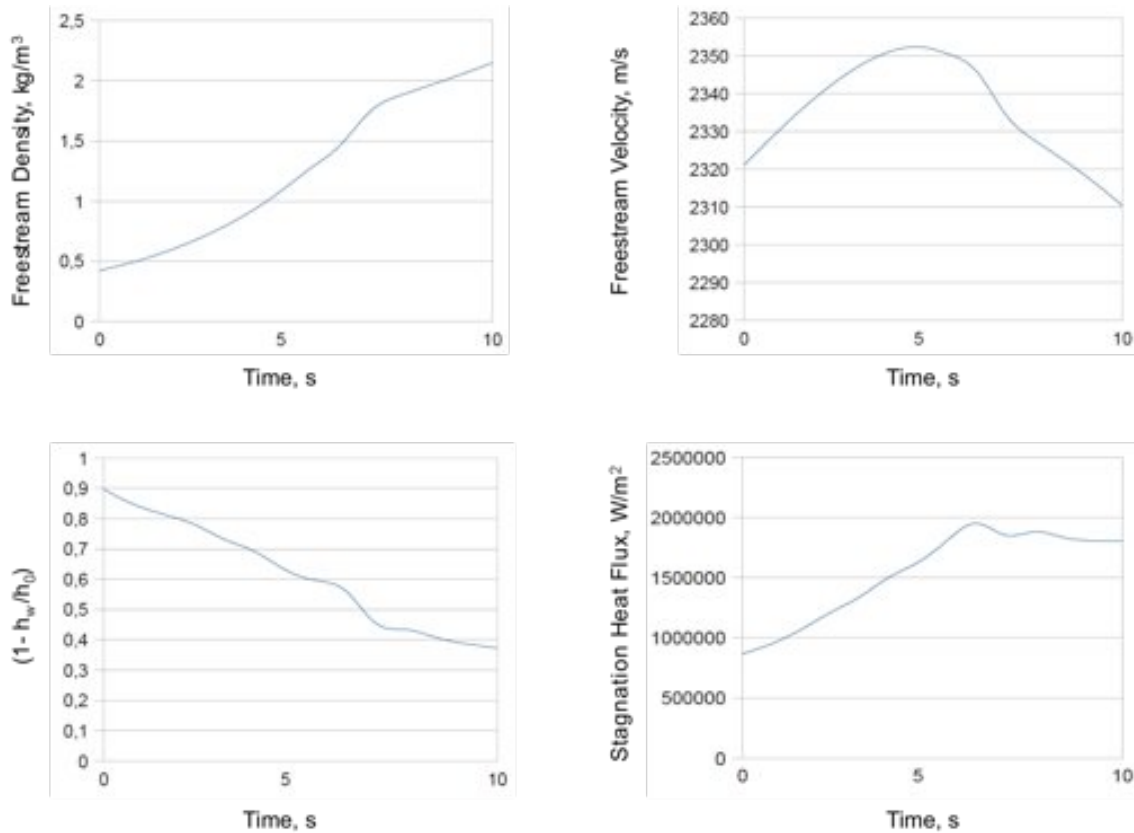


Figure 21. Variation of (a) freestream density, (b) freestream velocity, (c) ratio of wall to total enthalpy and (d) stagnation heat flux for a 10-second descent from 50 km at Mach 7.

Fluid-structure interaction approach

A strongly-coupled approach was used to model the fluid-structural interactions during the atmospheric descent. The commercial RANS code ANSYS CFX was used to model the fluid dynamics while the ANSYS Structural FEM solver was used to model the thermal-structural behaviour of the solid. Quasi-two-way fluid-structure-interactions were modelled using the ANSYS environment in which heat flux, skin friction and pressure loads were passed from the CFD solver to the FEM solver and only surface temperature distributions but not the structural deformations were passed back to the CFD solver during the transient modelling of the descent.

CFD and FEM solution domains

Fluid and solid domains were defined and meshed to represent the HIFiRE-0 vehicle in flight. In this case an axisymmetric approach was taken by assuming a zero angle of attack for the vehicle during its descent. The software though required the definition of a finite slice of the vehicle and for these calculations a 5° slice was used for each of the fluid and solid domains. The information at the boundary nodes of the fluid domain were automatically interpolated onto the equivalent boundary nodes of the solid domain and vice versa during the transient iterations. The solid model domain used for the FEM calculations is shown in Figure 8 with detail of the mesh in the region of the solid nose cone tip. The remainder of the wall of the nose cone and instrument can was simply modelled as a thin shell.

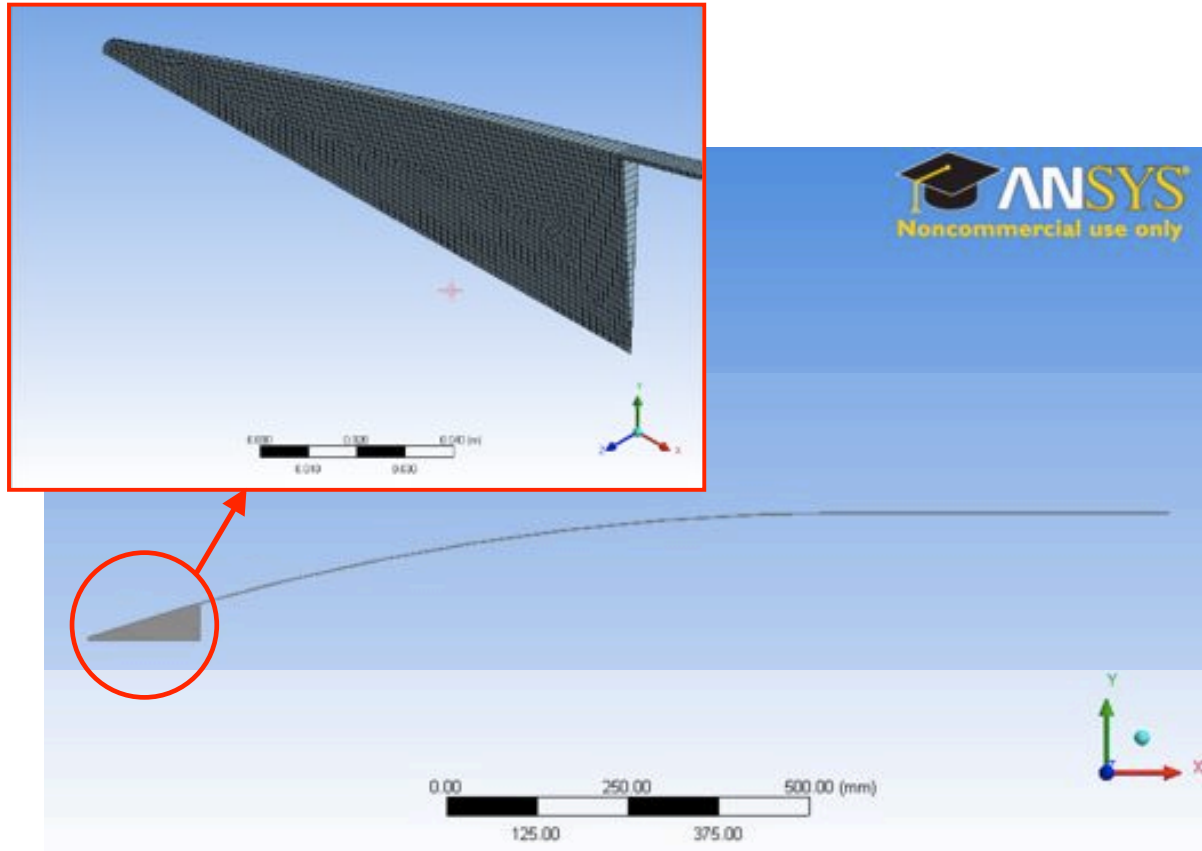


Figure 22. Solid model of the vehicle showing detail of the nose cone tip for the 3522 element FEM mesh.

Mesh independence for the FEM domain was established using transient simulations performed at constant altitude to reduce solution time. Four solid meshes of 2021, 3522, 7591 and 10006 elements were examined. Calculated values of surface temperature and deformation were found to be independent of the mesh for the chosen 3522 element mesh.

As stated, the commercial RANS code ANSYS CFX was used to model the fluid dynamics. As with the FEM domain, a quasi-2D-axisymmetric domain was built using a 5° slice. In order to adequately solve the boundary layer, the first node distance was maintained at $1\text{E-}6\text{m}$ from the wall. The y^+ value varied from 0.008 at the tip of nose cone to 0.208 at the trailing edge. A height ratio of 1.1 was maintained to keep elements in the normal-to-surface direction small enough to adequately resolve the boundary layers. Turbulence was modelled using a $k-\omega$ based shear stress transport model, with an assumption of 1% turbulent intensity in the inflow conditions.

As with the FEM solution, mesh independence for the CFD was established using transient simulations performed at constant altitude to reduce solution time. Four 2D-axisymmetric fluid meshes of 29151, 58539, 117394 and 235104 elements were examined.

Heat flux and y^+ values at a point on the thin wall of the nose cone were used to assess the mesh dependence. The maximum deviation between the finest and coarsest mesh was 1.42% for heat flux and 0.65% for the y^+ value. The chosen mesh (117394 elements), shown in Figure 23, had 0.21% deviation from the heat flux and 0.65% the y^+ value of the finest mesh.

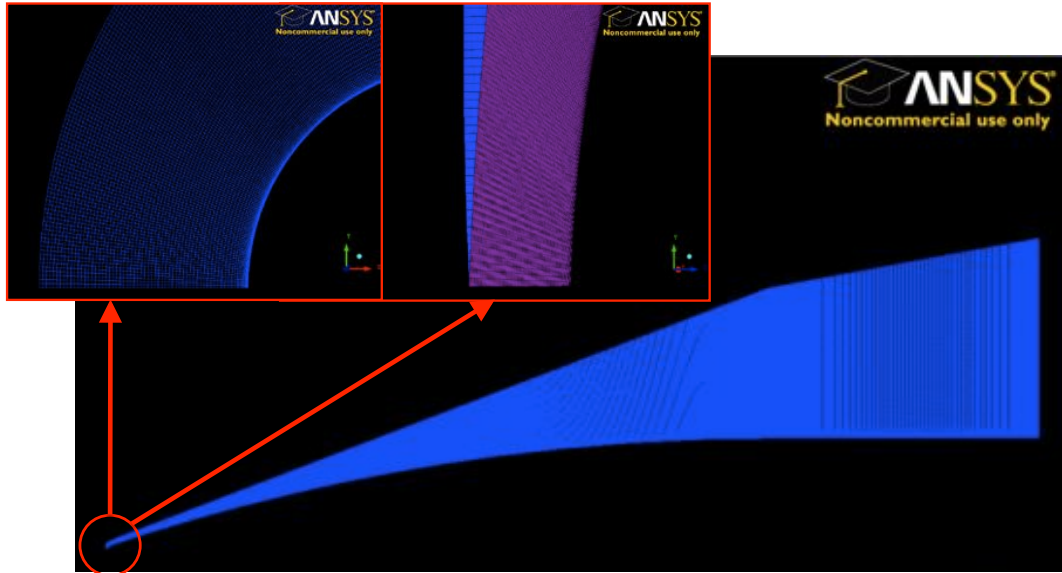


Figure 23. CFD domain used to model the flow field over the HIFiRE-0 vehicle. Inserts show detail of the mesh in the vicinity of the nose cone tip.

Transient FSI Solutions

The ANSYS Workbench commercial environment has been used to perform the FSI simulations. Within Workbench the RANS code ANSYS CFX was used to model the fluid dynamics while the ANSYS Structural FEM solver was used to model the thermal-structural behaviour of the solid. While the pressure-based CFX solver is not ideal for hypersonic applications it has been previously demonstrated for external aerodynamic simulations with some success (Deepak et al. 2008, Menezes et al. 2003). The approach used in the FSI calculations is detailed in a related paper (Neely et al. 2011). Freestream boundary conditions for the flow field were taken from the nominal Mach 7 HyShot 2 trajectory (Smart et al. 1996) as this previous mission used a matching two-stage Terrier-Orion booster.

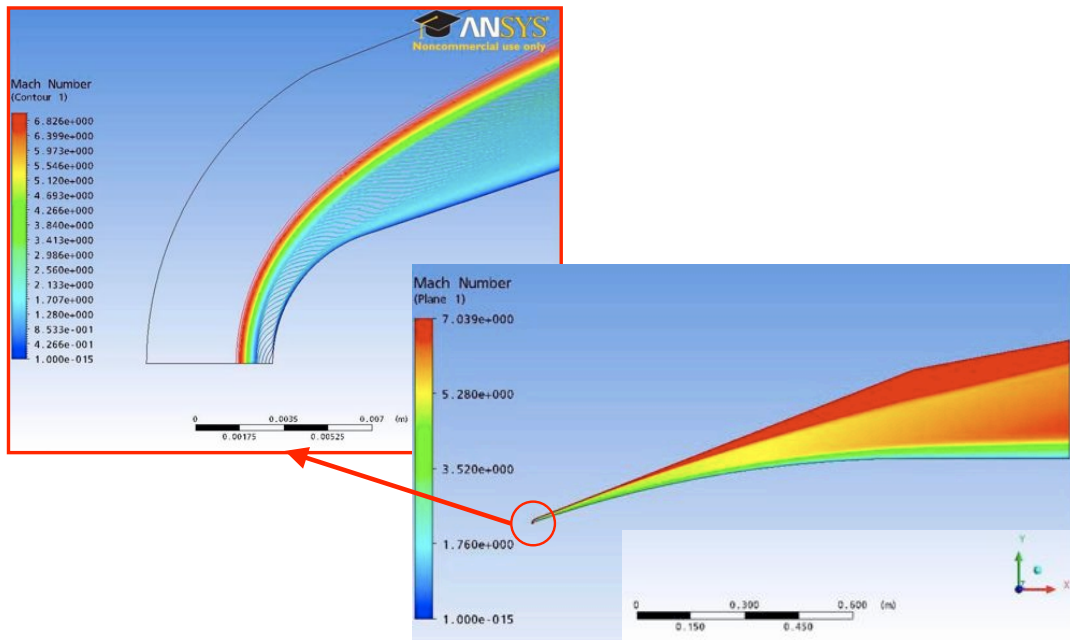


Figure 24. CFD flow field solution showing detail of Mach number distribution near the tip of the nose cone at 50 km altitude and a flight speed of 2321 m/s.

The FSI solution provides full volume distributions of the material temperature in the nose cone (Figure 25a) as well as distributions of stress (Figure 25b) and strain. The structural loads result from both the aerodynamic and the aerothermal loads. This data can be used by the designers to check the structural integrity and design efficiency of the vehicle as well as assist in the selection of the thermal paint types and locations of interest.

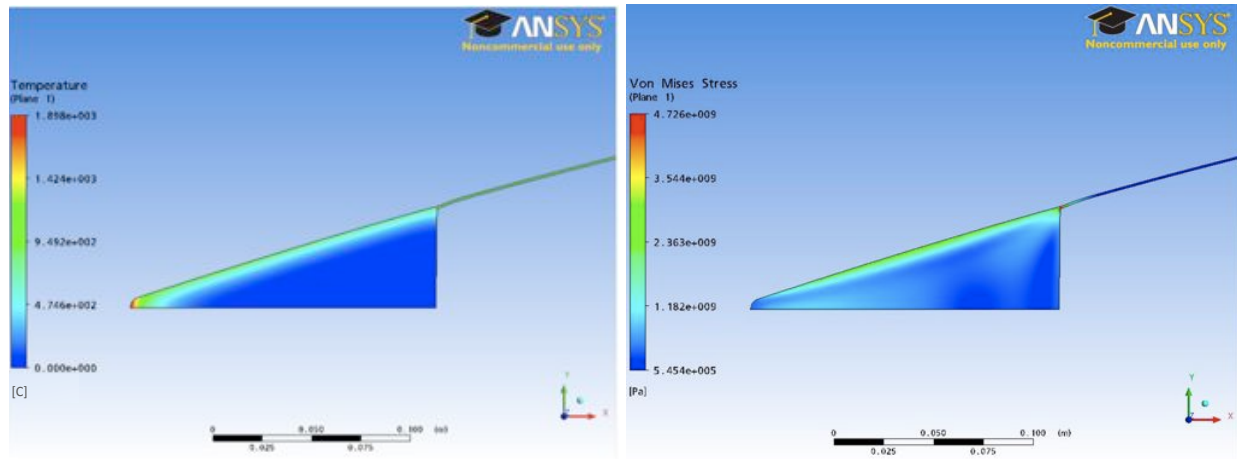


Figure 25. (a) Temperature distribution, °C and (b) stress distribution, Pa in the nose cone tip after a 10-second descent from 50 km to 28 km.

Full histories of each of these quantities are calculated throughout the solid volume of the vehicle structure. Figure 26 shows the evolution of surface temperature during the 10-second descent through the thickening atmosphere from 50 km to 28 km at three locations along the vehicle; at the stagnation point at the nose cone tip, at a point on the thin nose cone shell and on the wall of instrument can at the back of the vehicle. As may be expected, significant differences in the temperature histories are apparent due both to the growth of the thermal boundary layer along the vehicle and to the reduced heat capacity in the latter sections due to the thin wall.

These initial calculations have only modelled the descent of the vehicle and do not account for the additional heating of the nose cone and instrument can during the ascent through the atmosphere after launch. To provide an input to the transient paint calibrations for comparison with the final paint colours on the recovered vehicle, it will be necessary to repeat the transient FSI simulations for both the ascent and descent using the actual trajectory flown by the vehicle as recorded by the flight telemetry.

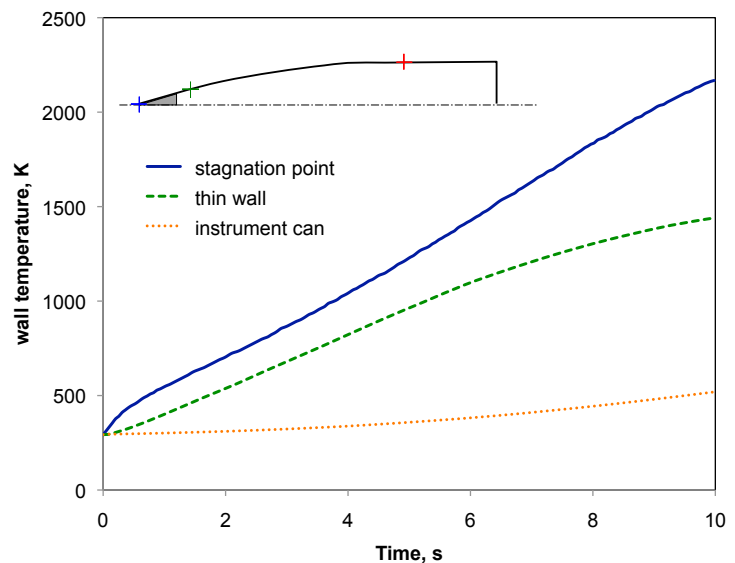


Figure 26. Surface temperature histories at three locations along the vehicle during the 10-second descent from 50 km to 28 km.

Predictions of the temperature distributions across the vehicle structure are required to select both regions of interest and appropriate thermal paints to apply. These transient simulations are also then used to provide calibration data for the paints and heating information for interpretation of post-flight colour change.

For the present work a combination of computational fluid dynamics (CFD) and finite element analysis (FEM) is being used to model the two-directional fluid-structure interaction (FSI) between the hypersonic flow around the vehicle and the structure of the nose cone and instrument can. Transient simulations have been performed over the segments of the vehicle's expected ascent and descent trajectory within the atmosphere to predict the distribution of surface temperature history on the nose cone and instrumentation can resulting from aerothermodynamic heating.

The FSI solution provides full volume distributions of the material temperature and resulting structural loads in the vehicle (Figure 27 and Figure 28). The structural loads result from both the aerodynamic and the aerothermal loads. This data can be used by the designers to assess the structural integrity and design efficiency of the vehicle as well as assist in the selection of the thermal paint types and locations of interest.

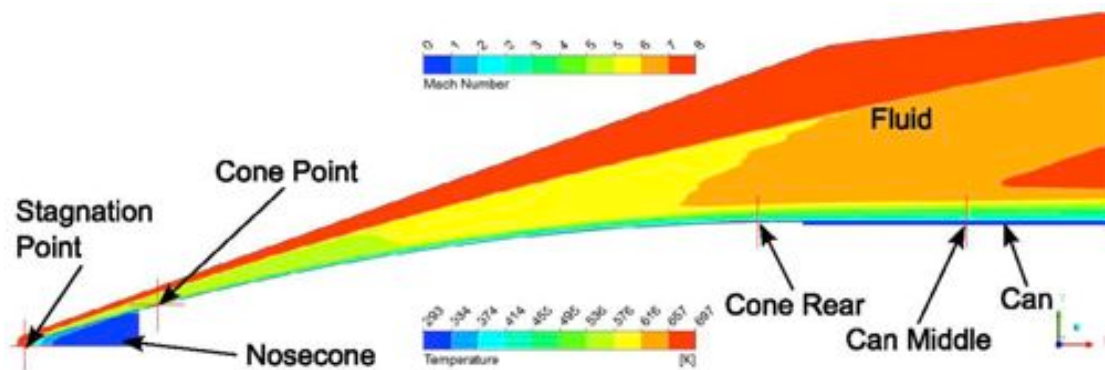


Figure 27. Mach number distribution in the external flow and temperature distribution in the HIFiRE-0 vehicle structure calculated from transient FSI simulations.

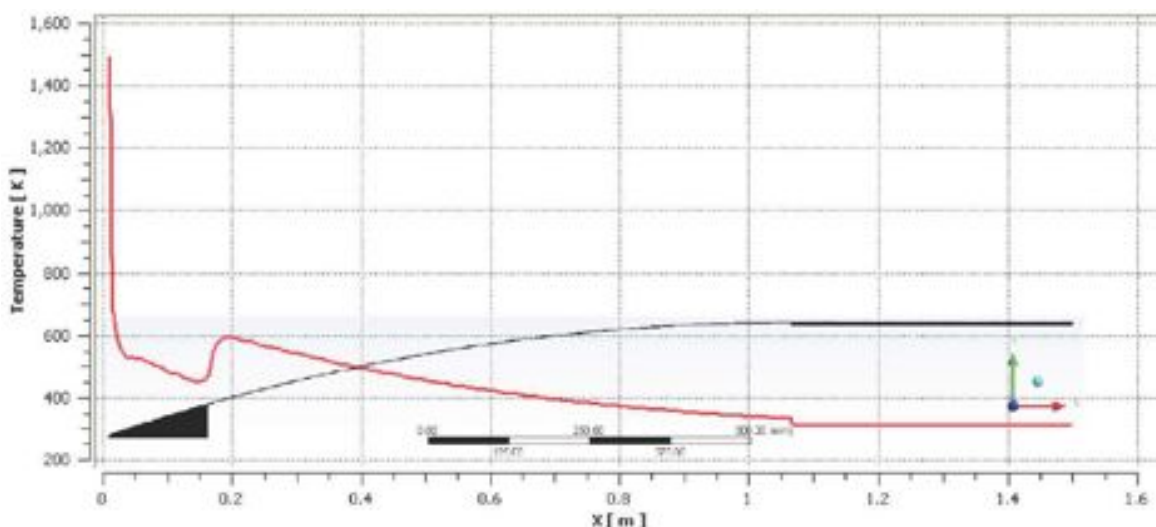


Figure 28. Temperature distribution along the surface of the HIFiRE-0 vehicle structure after descent through the atmosphere.

Flight Testing of the Permanent-Change Thermal Paints

HIFiRE-0 Flight Test Vehicle

HIFiRE-0 (Odam *et al.* 2009) was the first test flight flown under the Hypersonic International Flight Research Experimentation (HIFiRE) project, which is a joint initiative between the Australian Defence Science & Technology Organisation (DSTO) and the United States Air Force in collaboration with Australian and US universities and industries (Dolvin 2008). HIFiRE-0 was launched from the Woomera test range in South Australia in May 2009 and was designed to nominally follow a similar trajectory to that flown by the successful HyShot 2 experiment, which reached an apogee in excess of 300 km using a two stage Terrier-Orion solid rocket booster and then reentered the atmosphere at a Mach number of just over 7.5 as it descended, still attached to the expended second-stage rocket motor (Smart *et al.* 2006).

HIFiRE-0 was a risk-reduction engineering test flight and as such carried no scientific payload. The HIFiRE-0 vehicle consisted of a thin stainless steel ogive nose cone 1067 mm in length, permanently attached to a cylindrical aluminium instrumentation can which was itself permanently attached to the second stage Orion rocket motor. The tip of the nose cone consisted of two solid sections of stainless steel, modelled here as a single piece (Figure 29). The wall thickness of the stainless steel nose cone shell was 1 mm. The aluminium instrument can was modelled with a wall thickness 5 mm for the initial heating calculations described in this paper.

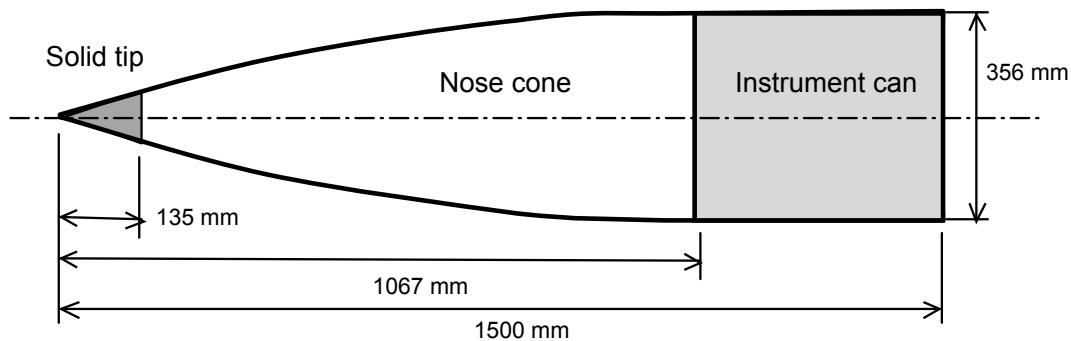


Figure 29. Layout of the modelled front section of the HIFiRE-0 vehicle.

Application of thermal paints to HIFiRE-0 vehicle

Figure 30 shows a range of views of the thermal paint scheme applied to the HIFiRE-0 test vehicle. Carefully selected patches of both single-change thermal paints, which pass through a single colour transition and multi-change thermal paints, which undergo multiple permanent colour transitions as they heat up, were applied to both exterior and interior surfaces of the stainless steel nose cone. Application of the paints on internal surfaces was used to avoid the erosion of the paint that is expected to occur on the external surface of the vehicle when it impacts the ground. The very thin wall thickness of the stainless steel nose cone will ensure that the internal surface temperature closely follows the external values. Longitudinal stripes were used to provide an indication of relative streamwise heating along the body. Patches of thermal paints with different ranges and responses were circumferentially distributed to ensure an enlarged dataset. These patches should nominally see the same heating histories due to the spin stabilization of the vehicle during its flight. This is analogous to a technique used in the gas turbine industry to obtain data from rotating turbine blades (Bird *et al.* 1998, Lempereur *et al.* 2008). Circumferential stripes of paint are used to assess the validity of this assumption by recording the uniformity of heating in this direction.

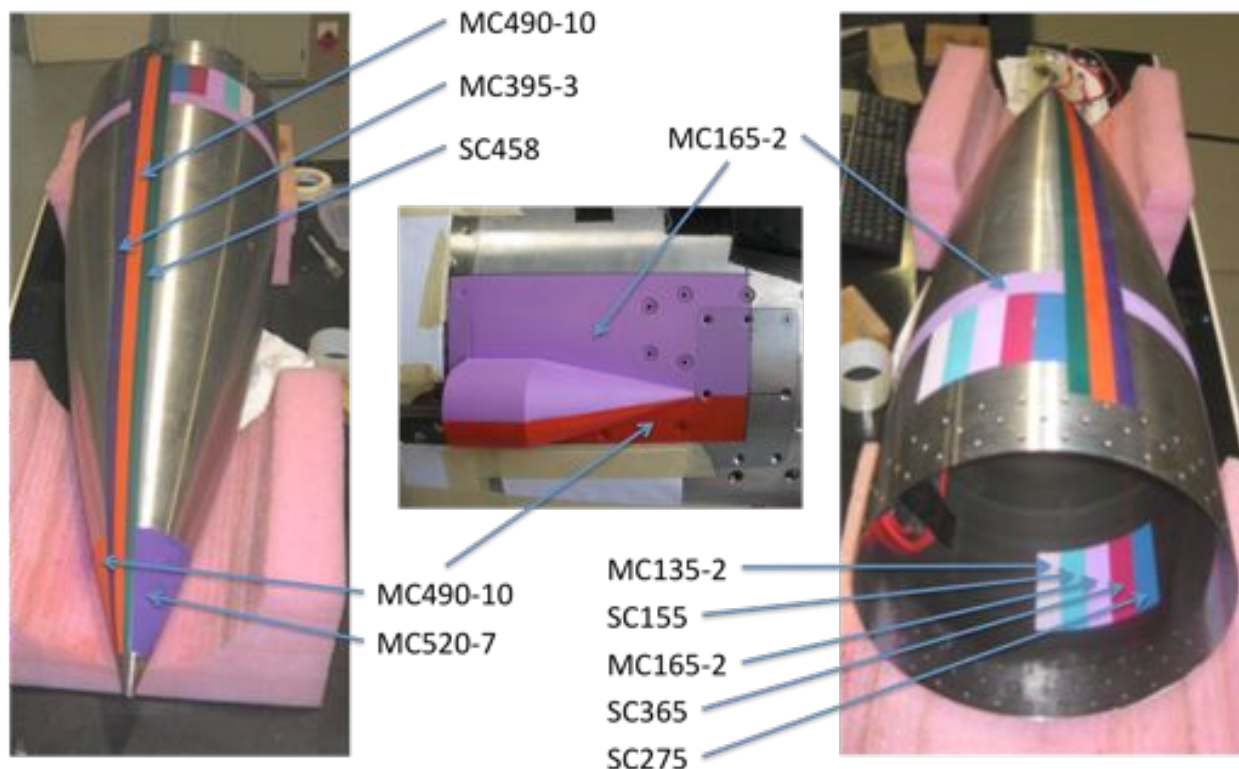


Figure 30. Paint scheme on the HIFiRE-0 vehicle showing patches of single-change and multi-change thermal paint on external and internal surfaces of the stainless steel nose cone and around the external camera mount on the instrument can (photos courtesy of DSTO).

Additionally, paint was applied around a dummy camera mount, which protrudes from the side of the payload (Figure 30). In this vicinity large gradients in aerodynamic heating and thus surface temperature will be produced by the shock/boundary layer interaction that will be induced by this three-dimensional compression surface and the streamwise corners between the mount and the fuselage. This degree of surface coverage would have been very expensive to achieve using discrete transducers in terms of instrumentation price, mass and wiring access and telemetry bandwidth requirements.

Figure 31 shows the painted HIFiRE-0 vehicle, assembled and attached to the Terrier-Orion booster rocket on the launch rail at the Woomera test range. Careful photographic records of the thermal paint coatings are desirable before launch to ensure that there has been no damage to or pre-flight thermal aging of the paints and to provide a reference baseline for later heating calculations.



Figure 31. HIFiRE-0 on the launch rail at the Woomera test range showing detail of the thermal paint coatings (photos courtesy of DSTO).

Post-flight analysis of paint response on HIFiRE-0

The main components of the HIFiRE-0 payload were recovered from the Woomera Test Range in August 2010 after spending 14 months in the desert. Despite the extended exposure to environmental elements, large sections of the applied paint patches were still visible on the vehicle components post recovery. Some environmental degradation was evident though, especially areas of corrosion on the aluminium parts (e.g. Figure 32).

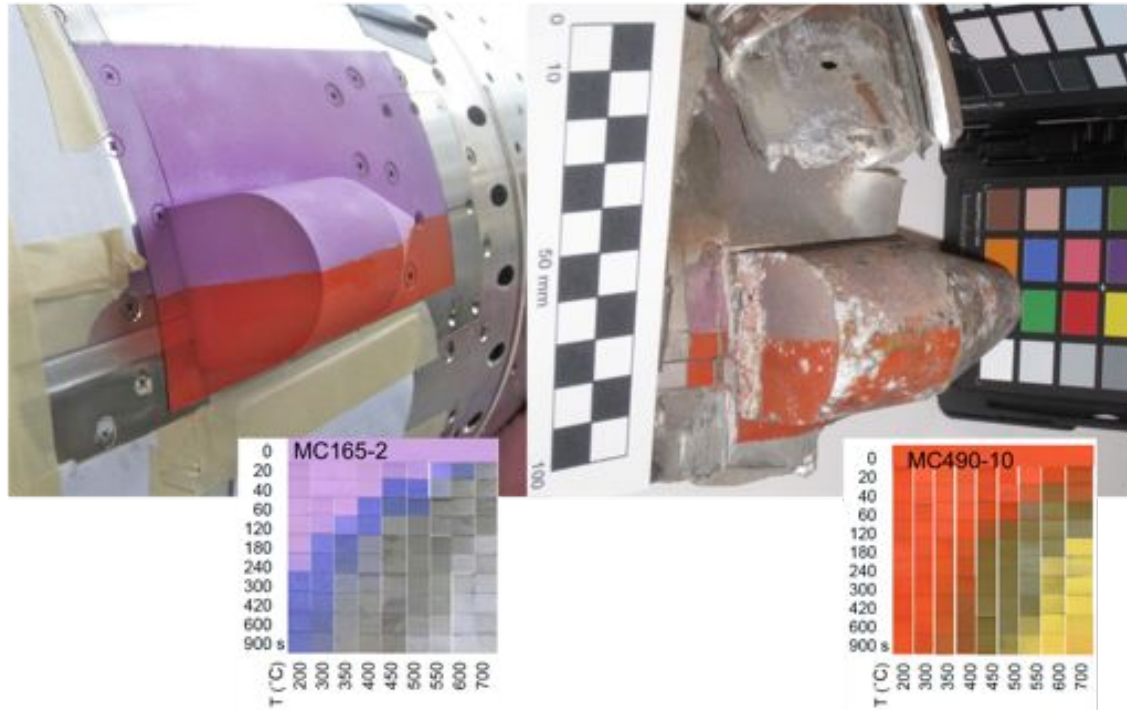


Figure 32. Views of the MC165-2 and MC490-10 permanent-change thermal paints applied to the dummy camera mount and its immediate surroundings including the frame of the patch antenna. (a) pre-flight paint condition and (b) post-flight paint condition showing significant colour change on the MC165-2 paint and corrosion of the aluminium dummy camera mount. Paint change schemes are shown for reference (photos courtesy of DSTO).

The components were carefully photographed using colour calibration cards to record any variation in the illumination source or digital camera settings. Comparisons of the before and after state of the paints in each location were made and will be described in detail in the full paper. Examples of the colour change in the vicinity of the dummy camera mount are shown in Figure 32 and Figure 33. More significant colour change is visible on the lower temperature MC165-2 thermal paint due to its lower colour transition temperature. Paint thicknesses were checked post flight using a Positector™ coating thickness gauge to determine what level of paint erosion had occurred (Figure 34(a)). The paint erosion varied between locations and substrate material. Paint bonding was far better on the aluminium components than on the polished stainless steel nose cone.



Figure 33. Close up of the patch antenna mount on the recovered debris from the HIFiRE-0 vehicle showing the colour change on the MC490-10 paint on the stainless steel mounting frame. Note that the dummy camera mount is no longer attached in these images. (photos courtesy of DSTO).

Calibration experiments using a specially designed electric-arc based heating rig (Figure 34(b)) are performed to reproduce the surface temperature histories experienced during flight. These histories are determined from the FSI calculations based on either the nominal (pre-flight) or actual (post-flight) trajectories. The calibration experiments for the HIFiRE-0 flight trajectory and the resultant colour changes performed using this rig will be reported in more detail in the final paper.



Figure 34. (a) Measurement of paint thickness post flight on recovered components.

The observed colour change on the recovered parts was compared with the component temperature histories predicted by the transient FSI simulations. Figure 35 shows an example of the temperature distribution around the patch antenna predicted by a transient simulation. In particular it confirms the existence of a region of high temperature along the overhanging edges of the stainless steel mounting frame that are in contact with the Duroid™ patch antenna. While the aluminium instrumentation can acts as a heat sink for the frame, the Duroid™ patch antenna acts as a thermal insulator and the section of the frame above it heats up more quickly thus causing the MC490-10 thermal paint colour change clearly visible in Figure 33. It is noted that this response is also visible in the tempering of the neighbouring uncoated steel.

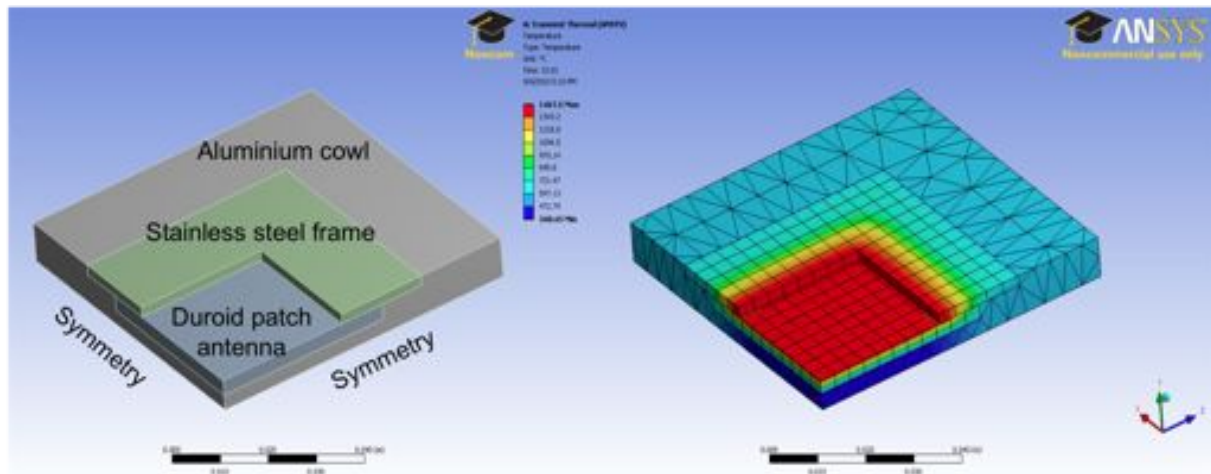


Figure 35. Transient simulation of the heating around the patch antenna mount on the aluminium instrumentation can. High levels of heating are visible along the overhanging edges of the stainless steel frame.

Summary

The overall objective of this research proposal is to develop and demonstrate a methodology for performing quantitative global temperature measurements on vehicle structures that have undergone hypersonic flight test.

The specific objectives were to:

- Investigate the paint chemistry and use spectroscopic measurements to determine the rate constants and activation energies of the colour-change reactions for the different paint mixtures. This had not previously been attempted for this class of paints as it has for TSPs. **The analysis techniques have been established and demonstrated and these have been reported here. Testing of the paint chemistry is ongoing and more complete results will be delivered in an addendum.**
- Investigate and develop an analytical model to predict an end paint colour from a predicted surface temperature history based on the Arrhenius constants. **The methodology has been established but is still under development as it is awaiting more complete data sets from the chemical characterisation.**
- Establishment of candidate heating histories representative of those experienced by the vehicle structure during hypersonic flight. **Numerically based techniques have been established and demonstrated to model the full transient heating of the vehicle across its trajectory. These methods can account for the fluid-thermal-structural interactions associated with the aerothermodynamic heating of the vehicle and its structural response. These simulations have successfully been applied to the critical portion of the atmospheric descent of the HIFiRE-0 payload. The techniques and initial simulations are described here. Extended modelling of the complete HIFiRE-0 trajectory is currently underway and the results will be used for calibration rig testing and the interpretation of the observed paint response.**
- Develop a controllable method of accurately reproducing predicted surface temperature histories on painted samples in the lab using CW laser heating. **Due to available power and OH&S restrictions an alternative method of reproducing transient heating histories representative of flight has been developed and demonstrated. This incorporates a computer-controlled high-power TIG welder to heat the sample via an electric arc.**
- Determine the overall levels of uncertainty of these measurements by directly comparing temperature history predictions based on final paint colour with the measured temperature histories used to induce the colour change. **This work is ongoing as data collection continues and more complete results will be delivered in an addendum.**

Additionally it was intended to pursue the following two objectives, which while sitting outside the basic science of the proposal will begin to address some of the engineering aspects of the technique:

- Test fly patches of paint under hypersonic test conditions (possibly on HIFiRE-0) to investigate the application methods, site selections and paint survivability in-flight and on impact. This will also provide an initial test case for post recovery handling and analysis of the painted surfaces. **This objective was achieved and the application of these paints to HIFiRE-0 is described. Very initial analysis of colour change on the recently recovered HIFiRE-0 vehicle is also briefly described. Paint has also been applied to and flown on the HIFiRE-1 vehicle, which has yet to be recovered.**
- Investigate the bonding of the paints to a range of materials and surface finishes under erosive high heat-flux conditions produced by the oxy-torch and strategies for the illumination and filming of internal painted surfaces for inclusion during flight tests. **Initial testing has begun but further work is required.**

Future Work

Much work remains to be done on quantifying the chemistry of the thermal paints to enable the prediction of the colour change resulting from a given surface temperature history. The findings of this ongoing study will be reported in more detail at the end of this calendar year. In addition the current research has identified a number of areas that require more detailed consideration.

- More work is required to understand the pressure dependence of the paint colour change. While work is ongoing to quantify this at sub-atmospheric conditions, an additional study should be undertaken to establish the behaviour of the paints at elevated pressures such as those in a combustion chamber. This will require the design, fabrication and instrumentation of an appropriate rig to produce conditions of elevated temperature and pressure simultaneously.
- While the calibration strategies described in this report will enhance our understanding of the paint behaviour and assist interpretation of the final paint colours, it is desirable to be able to perform a direct deduction of the surface temperature history from a recovered set of final paint colours via inverse methods. Dedicated research is required to come up with a suitable method to achieve this aim.
- The technique will continue to be perfected through lab-based calibration experiments and via application to further flight tests in the HIFiRE program and other international flights.
- Thought needs to be given to the design of dedicated aerothermodynamic flight experiments to leverage the global mapping capabilities of permanent-change thermal paints. These paints are well suited to the mapping of structural temperatures in areas of highly non-uniform heating such as in fin-fuselage junctions and other regions of shock boundary layer interaction as well as around reaction control jets and on combustor walls.
- A dedicated investigation on the bonding of the paints to a range of substrates, including non-metallic materials, and into the potentially adverse environmental weathering post-flight/pre-recovery must be performed to properly interpret the results from flight tests.
- Investigation and development of strategies for the illumination and filming of internal painted surfaces for inclusion during flight tests. There is a potential opportunity to place paints in view of existing cameras that are being flown on the HIFiRE series. This investigation should also include consideration of the application of the technique to the use of illuminated and imaged TSPs and thermal phosphors on internal vehicle surfaces.
- Dedicated testing of thermal paint coatings in facilities that can reproduce both the extreme transient heating and the fluid dynamic shear associated with the flight of a hypersonic vehicle. This will help provide an improved understanding of the bonding requirements for the paints and their resultant behaviour under these conditions. Consideration could be given to the use of arc-jet facilities or the testing of actively heated painted samples in appropriate hypersonic wind tunnels.

APPENDICES

Personnel Supported

Many people have contributed to this work either directly or indirectly. These include a number of undergraduate students, Phil Tracy, Wei Tjong (TJ), Katie Kruger, Lauren Armstrong, Harriet Cameron and Jack Appleton and a current graduate student Rishabh Choudhury. Bob Clark has provided technical assistance in the design and set-up of the electric-arc calibration rig and the oxy-acetylene torch calibration experiments.

Acknowledgements

DSTO is thanked for providing access to the HIFiRE-0 flight vehicle. UNSW and its Defence and Security Applications Research Centre (DSARC) has provided additional funding to support this work.

Publications Resulting from this Project

Neely AJ, Choudhury R, Riesen H, Paukner D, Odam J (2011) Measurement of Aerothermal Heating on HIFiRE-0, submitted for presentation at the AIAA 17th International Space Planes, Hypersonic Systems and Technologies Conference, San Francisco.

Neely AJ, Choudhury R, Paukner D (2011) Fluid-Thermal-Structural Interactions on a Hypersonic Fin, submitted for presentation at the AIAA 17th International Space Planes, Hypersonic Systems and Technologies Conference, San Francisco.

Neely AJ, Kruger KA, Riesen H, Yesil A & Odam J (2009) In-flight Mapping of Heating on a Hypersonic Nose Cone, AIAA 2009-7265, AIAA/DLR/DGLR 16th International Space Planes, Hypersonic Systems and Technologies Conference, Bremen.

Interactions

A number of important interactions have resulted from this funded project.

- A Presentation of aspects of the work at the AIAA/DLR/DGLR 16th International Space Planes, Hypersonic Systems and Technologies Conference, Bremen at the end of 2009.
- Participation in the Australian Government funded (2010-2012) SCRAMSPACE project to design instrument and fly a research payload to investigate scramjet-based access to space.
- Continuing participation in the HIFiRE series of test flights.
- Negotiation with DLR of participation in the SHEFEX 2 flight test.
- Discussions of work in a number of undergraduate and postgraduate courses and at a range of public forums for schools and the general public.

Allocation of the Budget

AOARD grant FA2386-09-1-4025 (2009-10) provided US\$35 000 towards the project.

US\$31 818 (AU\$40 061) was available for spending on the project after the deduction of University overheads.

This balance was used to purchase the following items:

• Miller Dynasty 350 industrial TIG welder and accessories	\$11 048
• National Instruments data acquisition and control components	\$13 129
• Data logging workstation	\$5 025
• Thermax permanent-change thermal paints	\$3 471
• Additional consumables (PMA solvent, KBr disks etc)	\$1 336
• Air brushes and portable compressor	\$750
• Travel for personnel to DSTO Brisbane for application and analysis of paints	\$1 480
• Contribution to support of CFD postdoctoral research assistant	balance

References

Allen, H.J. and Eggers, A.J., Jr, "A study of the motion and aerodynamic heating of ballistic missiles entering the earth's atmosphere at high supersonic speeds," NACA Report 1381, 1958.

Allison, S.W., Gillies, G.T., "Remote thermometry with thermographic phosphors: Instrumentation and applications", *Review of Scientific Instruments*, 68, 7, 1997, pp. 2615-2650.

Balter-Peterson, A., Frankmifsud, B. Love, W, "Arc jet testing in NASA Ames Research Center thermophysics facilities", AIAA-1992-5041, 1992.

Banks, D.W., van Dam, C.P., H. J. Shiu, H.J. and Miller, G.M., "Visualization of In-Flight Flow Phenomena Using Infrared Thermography", NASA TM-2000-209027, 2000.

Beckwith, I.E. and Miller, C.G., "Aerothermodynamics and Transition in High-Speed Wind Tunnels at NASA Langley," *Annual Review of Fluid Mechanics*, Vol. 22, 1990, pp. 419-439.

Bird, C., Mutton, J.E., Shepherd, R., Smith, M.D.W. and Watson, H.M.L., "Surface Temperature Measurement in Turbines", AGARD-CP-598, 1998.

Bown NW, Cain TM, Jones TV, Shipley PP and Barry B (1994) In Flight Heat Transfer Measurements on an Aero-Engine Nacelle, ASME 94-GT-244.

Cowling, J.E., King, P. and Alexander, A.L., "Temperature-Indicating Paints, *Industrial and Engineering Chemistry*, Vol. 45, No. 10, 1953, pp. 2317-2320.

Deepak NR, Ray T and Boyce RR (2008) Evolutionary Algorithm Shape Optimization of a Hypersonic Flight Experiment Nose Cone, *Journal of Spacecraft and Rockets*, Vol. 45, No. 3, 428-437.

Del Vecchio A, Marino G, Thoemel J, Ratti F and Gavira Izquierdo J (2009) EXPERT – The ESA Experimental Re-Entry Vehicle: Overview of the Experiments and Payloads qualified and accepted for the flight, AIAA 2009-4221, 39th AIAA Fluid Dynamics Conference, San Antonio, Texas.

Diakunchak, I.S., Gaul, G.R., McQuiggan, G. and Southall, L.R., "Siemens Westinghouse Advanced Turbine Systems Program Final Summary," *Journal of Engineering for Gas Turbines and Power-Transactions of The ASME*, Vol. 126 No. 3, 2004, pp. 524-530.

Dolvin DJ (2009) Hypersonic International Flight Research and Experimentation Technology Development and Flight Certification Strategy, AIAA 2009-7228, 16th AIAA / DLR/ DGLR International Conference on Space Planes and Hypersonic Systems and Technologies, Bremen.

Dolvin, D.J., "Hypersonic International Flight Research and Experimentation (HIFiRE) Fundamental Sciences and Technology Development Strategy", AIAA-2008-2581, 2008.

Edney, B., "Anomalous heat transfer and pressure distributions on blunt bodies at hypersonic speeds in the presence of an impinging shock," FFA Report 115, The Aeronautical Research Institute of Sweden, 1968.

Feist, J.P. and Heyes, A.L., "Thermographic phosphor thermometry for film cooling studies in gas turbine combustors", *Proceedings of the IMechE, Part A: Journal of Power and Energy*, Vol. 217, No. 2, 2003, pp. 193-200.

Foelsche, R., Leylegian, J., Betti, A., Chue, R., Marconi, F., Beckel, S., Tyll, J., Charletta, R. and Bakos, R., "Progress on the Development of a Freeflight Atmospheric Scramjet Test Technique," AIAA-2005-3297, 2005.

Foley, J.D., van Dam, A., Feiner, S.K. and Hughes, J.F., "Computer Graphics: Principles and Practise," 2nd Edition, Addison-Wesley Publishing Company, New York, 1996.

George WO, McIntyre PS, Infrared Spectroscopy, Chichester West-Sussex, Wiley, London, 1987.

Goynes, C.P., Hall, C.D., O'Brien, W.F., and Schetz, J.A., "The Hy-V Scramjet Flight Experiment", 14th AIAA/AHI Space Planes and Hypersonic Systems and Technologies Conference, AIAA-2006-7901, 2006.

Griffin, A., Kittler, J., Windeatt, T. and Matas, G., "Techniques for the Interpretation of Thermal Paint Coated Samples," *Proceedings of the 1996 Conference on Pattern Recognition*, IEEE, New York, 1996, pp. 959-963.

Ho, S-Y and Paull A., "Coupled thermal, structural and vibrational analysis of a hypersonic engine for flight test", *Aerospace Science and Technology*, No. 10, 2006, pp. 420-426.

Horvath TJ, Tomek DM, Berger KT, Splinter SC, Zalameda JN, Krasa PW, Schwartz RJ, Gibson DM, Tietjen A (2010) The HYTHIRM Project: Flight Thermography of the Space Shuttle During Hypersonic Re-entry, AIAA 2010-241, 48th AIAA Aerospace Science Meeting Conference, Orlando FL.

Huebner, L.D., Rock, K.E., Ruf, E.G., Witte, D.W. & Andrews E.H., "Hyper-X flight engine ground testing for flight risk reduction", *Journal of Spacecraft and Rockets*, Vol. 38, No. 6, pp. 844-852.

Iliff, K.W., Shafer, M., "A comparison of hypersonic vehicle flight and prediction results", AIAA-93-0311, 1993.

Ireland, P.T, Neely, A.J., Gillespie, D.R.H and Robertson, A.J., "Turbulent heat transfer measurements using liquid crystals", *International Journal of Heat and Fluid Flow*, Vol. 20, 1999, pp. 355-367.

Ireland, P.T. and Jones, T.V., "Liquid crystal measurements of heat transfer and surface shear stress," *Measurement Science and Technology*, Vol. 11, No. 7, 2000, pp. 969-986.

Jenkins, D.R. and Landis, T.R., "Hypersonic: The story of the North American X-15," Specialty Press, 2003.

Jones, R.A. and Hunt, J.L., "Use of temperature-sensitive coatings for obtaining quantitative aerodynamic heat-transfer data," *AIAA Journal*, Vol. 2, No. 7, 1964, pp.1354-1356.

Kafka, P.G., Gaz, J. and Yee W.T., "Measurement of Aerodynamic Heating of Wind-Tunnel Models By Means of Temperature-Sensitive Paint," *Journal Of Spacecraft and Rockets*, Vol. 2, No. 3, 1965, pp. 475-477.

Kaminski, C.F., Hughes, I.G., Lloyd, G.M. and Ewart, P., "Thermometry of an oxy-acetylene flame using multiplex degenerate four-wave mixing of C_2 ", *Applied Physics B* 62, 1996, pp. 39-44.

Khalid A.H. and Kontis, K., "Thermographic Phosphors for High Temperature Measurements: Principles, Current State of the Art and Recent Applications", *Sensors*, 8, 2008, pp. 5673-5744.

Kojima, F., Fukuda, S., Asai, K. and Nakakita, K., "Identification of Time and Spacial Varying Heat Flux from Surface Measurements based on TSP technology", Proceedings of the SICE Annual Conference.

Lalanne, T. and Lempereur, C., "Color recognition with a camera: a supervised algorithm for classification", ONERA report, 2001, pp. 198-204.

Lempereur, C., Andral, R. and Prudhomme, J.Y., "Surface temperature measurement on engine components by means of irreversible thermal coatings", *Measurement Science and Technology*, vol. 19, Aug, 2008, pp. 1-11.

Leonard, C.P., Amundsen, R.M. and Bruce, W.E., III, "Hyper-X Hot Structures Design and Comparison With Flight Data," AIAA-2005-3438, 2005.

Liu, T. and Sullivan, J.P., "Pressure and Temperature Sensitive Paints", Springer, 2005.

Longo JMA (2009) Present Results and Future Challenges of the DLR SHEFEX Program, AIAA 2009-7226, 16th AIAA/DLR/DGLR International Space Planes and Hypersonic Systems and Technologies Conference, Bremen.

Matthews, R.K. and Key, J.C., Jr, "Comparison of Wind-Tunnel and Flight-Test Heat-Transfer Measurements on a Pylon-Mounted Store," *Journal of Aircraft*, Vol.14, No.6, 1977, pp. 565-568.

McClinton, C.R., "X-43-Scramjet Power Breaks the Hypersonic Barrier," Dryden Lectureship in Research for 2006, AIAA-2006-1, 2006.

Mehryar, R., Giovannini A. and Cazin, S., "Paint Effects on the Advanced Quantitative Infrared Thermography Applied to Jet Impacts", Report for Institut de Mecanique des Fluides, 2006.

Menezes V, Saravanan S, Jagadeesh G, and Reddy KPJ, (2003) Experimental Investigations of Hypersonic Flow over Highly Blunted Cones with Aerospikes, *AIAA Journal*, Vol. 41, No. 10.

Metallic Materials and Elements for Aerospace Vehicle Structures, US DOD, AMSC N/A FSC 1560, MIL-HDBK-5H, 1 December 1998.

Nash, D.H. and Dempster, I.R., "Modelling the sources of cracking of aircraft compressor vanes rings," *Engineering Failure Analysis*, Vol. 12, No. 5, 2005, pp. 699-710.

Neely AJ, Choudhury R, Paukner D (2011) Fluid-Thermal-Structural Interactions on a Hypersonic Fin, submitted for presentation at the AIAA 17th International Space Planes, Hypersonic Systems and Technologies Conference, San Francisco.

Neely AJ, Kruger KA, Riesen H, Yesil A & Odam J (2009) In-flight Mapping of Heating on a Hypersonic Nose Cone, AIAA 2009-7265, AIAA/DLR/DGLR 16th International Space Planes, Hypersonic Systems and Technologies Conference, Bremen.

Neely, A.J. and Tjong W.C., "Calibration of Thermal Paints for Hypersonic Flight Test", AIAA-2008-2664, 2008.

Neely, A.J. and Tracy P.J., "Transient response of thermal paints for use on short-duration hypersonic flight tests", AIAA-2006-8000, 2006.

Neumann, R.D. and Hayes, J.R., "Introduction to aerodynamic heating analysis of supersonic missiles," *Tactical Missile Aerodynamics: Prediction Methodology*, edited by M.R. Mendenhall, Progress in Astronautics and Aeronautics Series, AIAA, Washington DC, 1992, p. 421-481.

Odam J, Paull A, Alesi H, Hunt D, Paull R, Pietsch R (2009) HIFiRE 0 Flight Test Data, AIAA 2009-7293, 16th AIAA/DLR/DGLR International Space Planes and Hypersonic Systems and Technologies Conference, Bremen.

Odam, J., Neely, A.J., Stewart, B. and Boyce, R.R., "Heating analysis of a generic scramjet," AIAA-2005-3338, 2005.

Padgham, C.A. and Saunders, J.E., "The Perception of Light and Colour," G. Bell and Sons Limited, London, 1975.

Reed, R.D. and Watts, J.D., "Skin and structural temperatures measured on the X-15 airplane during a flight to a Mach number of 3.3," NASA TM-X-468, 1961.

Skoog, D.A., Holler, F.J. and Nieman, T.A., *Principles of Instrumental Analysis*, 6th ed., Brooks Cole, 2006, pp. 320-351.

Smart, M.K., Hass, N.E. and Paull, A., "Flight Data Analysis of the HyShot 2 Scramjet Flight Experiment," *AIAA Journal*, Vol. 44, No. 10, 2006, pp. 2366-2375.

Smith, N.S.A., "HyPAq: Software for the transient analysis of hypersonic vehicles in Abaqus", DSTO-TR-2236, Defence Science and Technology Organisation, Australia, 2008.

Stainback, P.C., "A visual technique for determining qualitative aerodynamic heat rates on complex configurations," NASA TN D-385, 1960.

Steinetz, B.M. and Dunlap, P.H., Jr., "Development of thermal barriers for solid rocket motor nozzle joints", *Journal of Propulsion and Power*, Vol. 17, No. 5, 2001, pp-1023-1034.

Stewart, B., Boyce, R., Neely, A. and Odam, J., "CFD Analysis of Nosecone Geometries and a Generic 2D Scramjet", AIAA-2005-3339, 2005.

Taniguchi, T., Sanbonsugi, K., Ozaki, Y. and Norimoto A., "Temperature Measurement of High Speed Rotating Turbine Blades Using a Pyrometer," ASME-GT2006-90247, 2006.

Tauber, M.E., "A Review of High-Speed, Convective, Heat-Transfer Computation Methods", NASA Technical Paper 2914, 1989.

Tertian R, *Principles of Quantitative X-Ray Fluorescence*, McGraw Hill, London, 1982.

Walker, S., Rodgers, F., Paull, A. and Van Wie, D.M., "HyCAUSE Flight Test Program", AIAA 15th International Space Planes, Hypersonic Systems and Technologies Conference, AIAA 2008-2580, 2008

Walker, S.H., Rodgers, F.C. and Esposito, A.L., "Hypersonic Collaborative Australia/United States Experiment (Hycase)," AIAA-2005-3254, 2005.